

Cardiolipin provides an essential activating platform for caspase-8 on mitochondria

Francois Gonzalvez,¹ Zachary T. Schug,¹ Riekelt H. Houtkooper,^{2,3} Elaine D. MacKenzie,¹ David G. Brooks,⁴ Ronald J.A. Wanders,^{2,3} Patrice X. Petit,⁵ Frédéric M. Vaz,^{2,3} and Eyal Gottlieb¹

¹Cancer Research UK, The Beatson Institute for Cancer Research, Glasgow G61 1BD, Scotland, UK

²Department of Clinical Chemistry and ³Department of Pediatrics, Laboratory Genetic Metabolic Diseases, University of Amsterdam, Academic Medical Center, Amsterdam 1105 AZ, Netherlands

⁴Division of Medical Genetics, Department of Medicine, University of Pennsylvania, Philadelphia, PA 19104

⁵Institut Cochin, Département de Génétique et Développement, Centre National de la Recherche Scientifique UMR 8104, Institut National de la Santé et de la Recherche Médicale U567 et Université Paris-Descartes, Paris 75014, France

Cardiolipin is a mitochondria-specific phospholipid known to be intimately involved with apoptosis. However, the lack of appropriate cellular models to date restricted analysis of its role in cell death. The maturation of cardiolipin requires the transacylase tafazzin, which is mutated in the human disorder Barth syndrome. Using Barth syndrome patient-derived cells and HeLa cells in

which tafazzin was knocked down, we show that cardiolipin is required for apoptosis in the type II mitochondria-dependent response to Fas stimulation. Cardiolipin provides an anchor and activating platform for caspase-8 translocation to, and embedding in, the mitochondrial membrane, where it oligomerizes and is further activated, steps that are necessary for an efficient type II apoptotic response.

Introduction

In mammalian cells, induction of apoptosis occurs via one of two distinct pathways: extrinsic or intrinsic. The extrinsic pathway responds to extracellular signals through death receptors at the plasma membrane (e.g., Fas and TNF-R1), whereas the intrinsic pathway is activated by intracellular stress. The intrinsic apoptotic cascade involves the release of apoptogenic factors (including cytochrome *c* and second mitochondria-derived activator of caspases [Smac]/Diablo) from mitochondria to the cytosol (Wang, 2001; van Loo et al., 2002). The release of apoptogenic factors requires permeabilization of the mitochondrial outer membrane, a process regulated by the Bcl-2 family of proteins, which comprises both proapoptotic (e.g., Bax, Bak, and Bid), and antiapoptotic (e.g., Bcl-2 and Bcl-xL) members (van Loo et al., 2002). As for extrinsically induced apoptosis, this can take the course of either one of two pathways depending on cell type. In type I cells, binding of the Fas death receptor induces the “death-inducing signaling complex” (DISC) on the

plasma membrane and activates a large amount of the initiator protease, caspase-8, which then cleaves and activates the executioner protease caspase-3. However, in type II cells, caspase-8 activation at the plasma membrane is limited, and the apoptotic signal relies on amplification from the mitochondrial apoptotic pathway (Scaffidi et al., 1998). Thus, in type II cells, after the activation of Fas at the plasma membrane, the extrinsic apoptotic pathway converges with the intrinsic one: caspase-8 cleaves Bid to its active form tBid, which induces mitochondrial outer membrane permeabilization and release of apoptogenic factors (Li et al., 1998; Luo et al., 1998).

Cardiolipin (CL), a phospholipid of the mitochondrial membrane, participates in several mitochondria-dependent apoptotic steps (Gonzalvez and Gottlieb, 2007), including the proapoptotic function of Bcl-2 proteins. CL can serve as a “docking site” for tBid on the mitochondrial membrane (Lutter et al., 2000) and is required for Bax activation and mitochondrial outer membrane permeabilization (Kuwana et al., 2002). By anchoring cytochrome *c* to the mitochondrial inner membrane, CL both facilitates the electron transport chain and encumbers cytochrome *c*

Correspondence to Eyal Gottlieb: e.gottlieb@beatson.gla.ac.uk

Abbreviations used in this paper: BMH, *Bis*-maleimido-hexane; CL, cardiolipin; DED, death effector domain; DISC, death-inducing signaling complex; MIB, mitochondria isolation buffer; MLCL, monolyso-CL; PARP, poly-ADP ribose polymerase; PC, phosphatidylcholine; PE, phosphatidylethanolamine; PI, propidium iodide; shRNA, short hairpin RNA; Smac, second mitochondria-derived activator of caspases.

The online version of this article contains supplemental material.

© 2008 Gonzalvez et al. This article is distributed under the terms of an Attribution–Noncommercial–Share Alike–No Mirror Sites license for the first six months after the publication date [see <http://www.jcb.org/misc/terms.shtml>]. After six months it is available under a Creative Commons License [Attribution–Noncommercial–Share Alike 3.0 Unported license, as described at <http://creativecommons.org/licenses/by-nc-sa/3.0/>].

release during apoptosis, which indicates that the complete release of cytochrome *c* requires the disruption of its interactions with CL (Shidoji et al., 1999; Ott et al., 2002). This is further supported by the fact that CL peroxidation, catalyzed by cytochrome *c*, is required for cytochrome *c* release from mitochondria (Kagan et al., 2005).

Despite the growing body of evidence implicating CL in apoptosis, the mechanism remains unresolved. To address the role of CL in apoptosis in a cellular system, Barth syndrome–derived lymphoblastoid cells and Barth syndrome–like cells were used. Barth syndrome (Barth et al., 1983; Kelley et al., 1991) is the only known human genetic disorder where alterations in CL metabolism are its primary cause (Hauff and Hatch, 2006; Gonzalez and Gottlieb, 2007). Barth syndrome is caused by mutations in *tafazzin* (Bione et al., 1996), which encodes a transacylase that directs CL maturation (Xu et al., 2006). After synthesis in mitochondria, CL is actively remodeled by tafazzin to generate its mature acyl form. CL contains four acyl chains. During CL maturation, phospholipase A removes one saturated acyl chain to generate monolyso-CL (MLCL) while tafazzin replaces it with an unsaturated acyl chain taken from phosphatidylcholine (PC), a process repeated until remodeling is complete (Xu et al., 2006). Therefore, in Barth syndrome, mature CL levels are low, whereas the levels of MLCL are high (Valianpour et al., 2005), making it a unique model for studying the role of mature CL in apoptosis in intact cells.

In this study, we show that CL is required for the type II extrinsic apoptotic pathway. In particular, CL is fundamental for the formation of an apoptotic signaling platform on the mitochondrial outer membrane supporting the recruitment, oligomerization, and processing of caspase-8. This step is critical for the release of apoptogenic factors from the mitochondrial intermembrane space. We show that unlike the type I response to Fas signaling, where caspase-8 is activated on the plasma membrane's DISC, in the type II response, caspase-8 relocates to the mitochondrial outer membrane, where its accumulation and activation relies on CL.

Results

Barth syndrome–derived lymphoblastoid cells resist induction of the extrinsic apoptotic pathway

Lymphoblastoid cells derived from Barth syndrome patients were used to study the role of CL in apoptosis. These cells were isolated from two unrelated patients and were immortalized *ex vivo* using Epstein-Barr virus infection. Both cell lines, termed DB105.2 and DB105.3, carry an inactive mutant form of *tafazzin*. Analysis of the CL levels in the lymphoblastoid cells showed low CL and high MLCL in the tafazzin-deficient lymphoblastoid cell lines when compared with the two control lymphoblastoid cell lines DB037 and DB015 (Fig. 1 A and not depicted). Moreover, the acyl chains of the different CL species in Barth syndrome–derived cells were less unsaturated, as determined by mass spectrometrical analysis, which showed a shift to higher *m/z* values within each cluster of CLs. In response to intrinsic death stimuli, such as etoposide or cisplatin, both control and

Barth syndrome lymphoblastoid cells underwent cell death to the same extent as measured by propidium iodide (PI) exclusion (Fig. 1 B). However, when treated with TNF- α or with anti-Fas antibody, a dramatic decrease in cell death was observed in the CL-deficient Barth syndrome–derived lymphoblastoid cells (Fig. 1 C), which prompted focus on the role of CL in Fas-mediated apoptosis. FACS demonstrated that cell surface-exposed Fas levels were unaltered in CL-deficient cells (Fig. S1, available at <http://www.jcb.org/cgi/content/full/jcb.200803129/DC1>). However, measurement of Annexin V binding to PI-negative cells (which is indicative of early apoptotic cells) showed a clear reduction in the response of Barth syndrome–derived lymphoblastoid cells to anti-Fas antibody compared with control cells (Fig. 1 D). These results indicate that CL-deficient lymphoblastoid cells are defective in the pathway that links the death receptor with the core apoptotic machinery.

Tafazzin knockdown reduces CL levels and increases resistance to apoptosis

Because CL is a mitochondria-specific phospholipid, it most likely plays a role in the mitochondria-dependent response to extrinsic apoptotic signals. This step, although dispensable in type I cells, is crucial for apoptosis of type II cells. It is of note that activated human lymphocytes present a type II response to Fas-mediated cell death (Zhang et al., 1996). To elucidate the involvement of CL in the type II cascade, HeLa cells were used because HeLa cells in which Bid was knocked down with Bid-specific siRNA showed a decrease in Fas-mediated cell death (Fig. S2, A and B, available at <http://www.jcb.org/cgi/content/full/jcb.200803129/DC1>) and reduced caspase-3–like activity (DEVDase), which indicates decreased apoptosome activity (Fig. S2 C). Moreover, Bcl-xL overexpression protected these cells from Fas-induced apoptosis (Fig. S2 D), further confirming that HeLa cells have a type II response to extrinsic apoptotic signals and that a Bcl-2–regulated, mitochondria-dependent step is required in these cells.

To generate a model for Barth syndrome, RNA interference was used to knock down tafazzin. Short hairpin RNA (shRNA)-encoding plasmids were constructed using either a *tafazzin*-specific sequence or a nonspecific shRNA control. HeLa cells were stably transfected, and cell clones (shTaz1, shTaz2, shCont1, and shCont2) were isolated. Quantitative PCR analysis showed that in shTaz1 and shTaz2 cells, the endogenous *tafazzin* RNA levels were reduced significantly (Fig. S3, available at <http://www.jcb.org/cgi/content/full/jcb.200803129/DC1>). A corresponding Western blot for endogenous tafazzin confirmed efficient knockdown of the protein (Fig. 2 A). Finally, the CL pattern of the tafazzin knockdown cells resembled that of Barth syndrome–derived lymphoblastoid cells (Fig. 2 B). Although the increase in MLCL is modest compared with Barth syndrome lymphoblastoid cells, a significant and comparable decrease in CL is evident in shTaz1 and shTaz2 cells with a dramatic loss of the major peaks of each cluster of CL species, which indicates severely defective maturation of CL (Fig. 2 B). Moreover, like Barth syndrome patients (Vreken et al., 2000), lack of *tafazzin* in HeLa cells has no effect on other major phospholipids (Fig. S4).

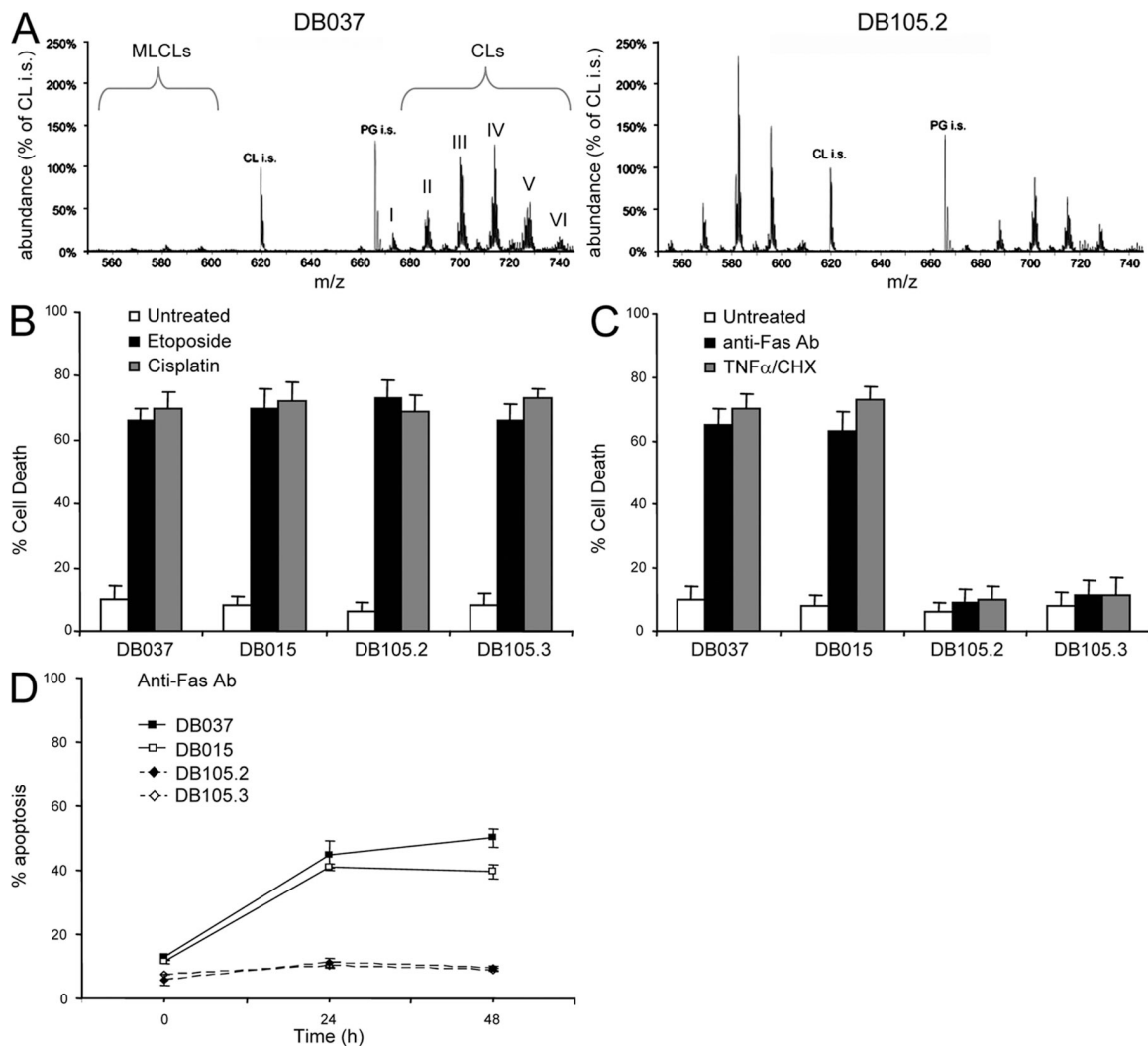


Figure 1. **Barth syndrome-derived lymphoblastoid cells are resistant to Fas-induced apoptosis.** (A) CL and MLCL profile of control (DB037) and Barth syndrome-derived (DB105.2) lymphoblastoid cells as determined by HPLC-MS. CL-i.s. and PG-i.s. are internal standards of known amounts of tetramyristoyl-CL and dimyristoyl-phosphatidylglycerol, respectively. The observed CL clusters (I–VI) are: I = 64 carbon atoms (likely 4 \times 16); II = 66 carbon atoms; III = 68 carbon atoms; IV = 70 carbon atoms; V = 72 carbon atoms (likely 4 \times 18); and VI = 74 carbon atoms. Each peak within a given cluster represents the saturation level of the acyl chains ranging from 0 (right) to the maximum 8 (left) double bonds. (B and C) Cell death of control (DB037 and DB015) and Barth syndrome-derived (DB105.2 and DB105.3) lymphoblastoid cells was analyzed by PI exclusion. Cells were treated with either intrinsic (B) or extrinsic (C) apoptotic stimuli for 24 h; 10 μ M etoposide or 25 μ M cisplatin were used as intrinsic stimuli, whereas anti-Fas antibody (0.5 μ g/ml) or recombinant TNF- α (20 ng/ml) together with cycloheximide (CHX; 20 μ g/ml) were used as extrinsic stimuli. (D) Cells were treated with anti-Fas antibody, and the kinetics of apoptosis was measured by FITC-annexin V staining of PI-negative cells. Error bars represent \pm standard deviation.

Similar to Barth syndrome lymphoblastoid cells, tafazzin knockdown HeLa cells were highly resistant to anti-Fas antibody-induced apoptosis (Fig. 2 C), and after Fas activation, they showed reduced DEVDase activity (Fig. 2 D). It is worth mentioning that, unlike Barth syndrome lymphoblastoid cells, tafazzin-knockdown HeLa cells were partially resistant to high doses of cisplatin or etoposide (unpublished data). This resistance to intrinsic cell death may be caused by the inactive p53 pathway of HeLa cells, and indicates that in these cells, an alternative, CL-dependent apoptotic pathway (potentially via an extrinsic loop) may be needed for efficient apoptosis induced by chemotherapeutic agents. To confirm that the Fas resistance is not caused by an off-target effect of the shRNA, silent mutations were introduced into the cDNA of human *tafazzin*, and

shTaz1 cells were transfected with this mutant to generate a revertant clone (shTaz1R). shTaz1R cells expressed tafazzin to a level comparable to the endogenous protein (Fig. 2 A), and CL levels were comparable to those of control cells (Fig. 2 B). Importantly, shTaz1R cells were highly sensitive to Fas-induced apoptosis (Fig. 2 C). Collectively, these data indicated that tafazzin is required for efficient Fas-induced apoptosis.

To confirm that loss of mature CL and not the loss of tafazzin itself is the cause of apoptosis resistance in tafazzin-deficient cells, tafazzin was transiently knocked down for 48 h using siRNA oligonucleotides. HeLa cells were transfected with a plasmid encoding a GFP-tafazzin fusion protein and with either nonspecific or *tafazzin*-targeting siRNAs. The GFP-tafazzin protein colocalized with the mitochondria-specific fluorescent dye

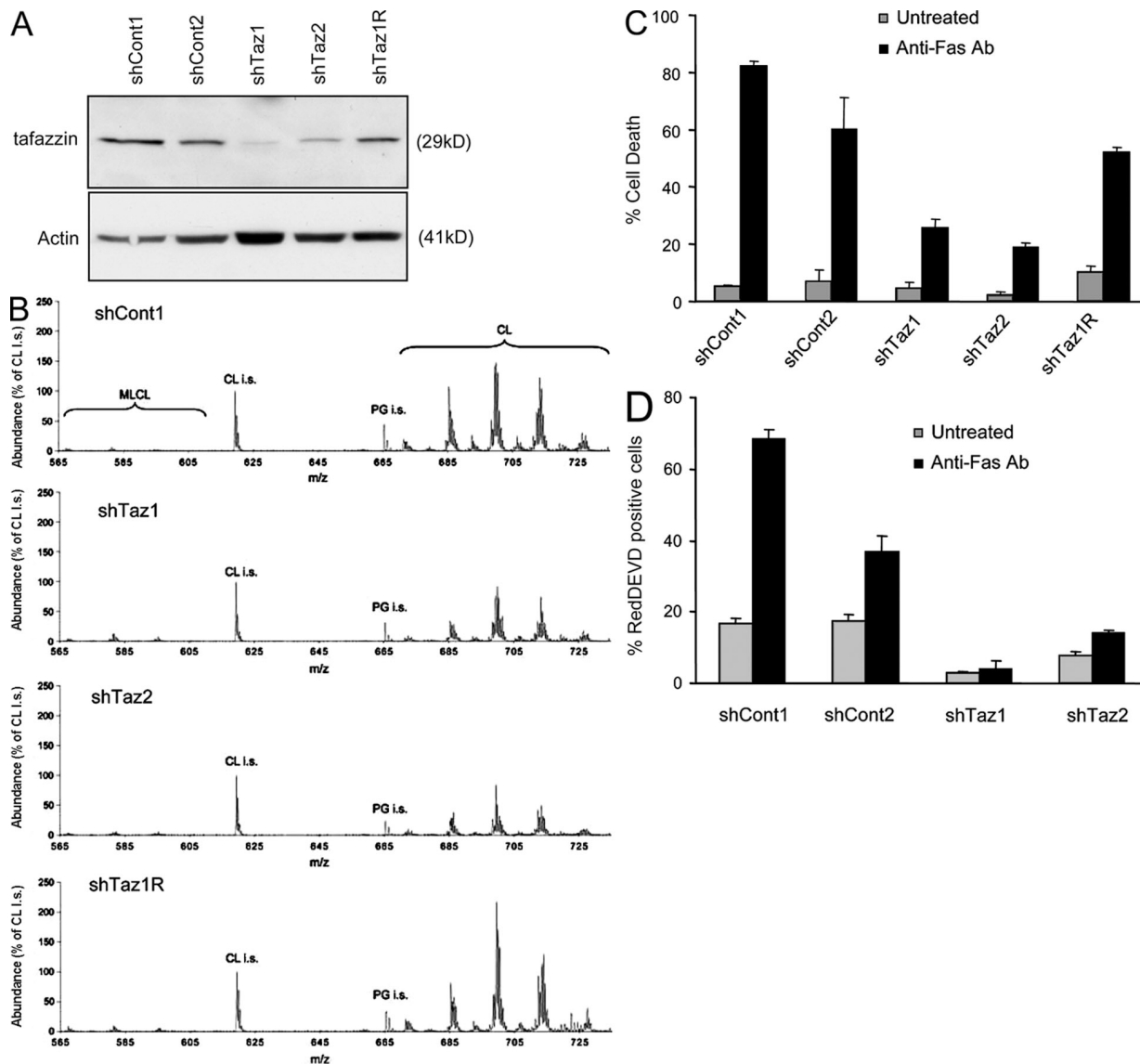


Figure 2. **Tafazzin-deficient HeLa cells display low CL levels and are resistant to Fas-induced apoptosis.** (A) Cells were stably transfected with either control shRNA-encoding plasmid (shCont1 and 2) or with *tafazzin*-targeting shRNA (shTaz1 and 2). Western blot analysis of endogenous tafazzin protein was used to confirm efficient knockdown of the protein. The shTaz1R clone was generated by reintroducing shRNA-resistant cDNA of tafazzin into shTaz1 cells. (B) The CL and MLCL profile of shCont1, shTaz1, shTaz2, and shTaz1R cells was analyzed as in Fig. 1 A. (C) Cell death analysis of the control, tafazzin-deficient, and revertant clone (shTaz1R) was performed 48 h after treatment with anti-Fas antibody. (D) DEVDase (caspase-3-like) activity of the indicated cells was performed 8 h after anti-Fas antibody treatment. Error bars represent \pm standard deviation.

tetramethyl rhodamine ethyl ester (TMRE), confirming its location in the mitochondria, and was efficiently knocked down in cells transfected with *tafazzin*-specific siRNA (Fig. S5 A, available at <http://www.jcb.org/cgi/content/full/jcb.200803129/DC1>). The efficiency of the *tafazzin*-targeting siRNA was further verified by Western blot analysis (Fig. S5 B). However, under these conditions, the CL pattern was unaltered in these cells, likely because of the low turnover of the lipids in these cells (Fig. S5 C). It was previously shown that, in the liver, the half-life of CL is the longest of all mitochondrial phospholipids (Landriscina et al., 1976). Importantly, transient depletion of tafazzin (without affecting the CL level) in HeLa cells did not modify the sensitivity of these cells to Fas-induced apoptosis (Fig. S5 D), ruling out a CL-independent role for tafazzin in the apoptotic process.

Cytochrome *c* release is impaired in Fas-induced CL-deficient cells

To understand the role of CL in Fas-induced apoptosis, the known steps of this pathway were investigated in tafazzin-knockdown cells. Caspase-3, which in type II cells requires cytochrome *c* release and apoptosome formation for its activation, showed a marked decrease in both autocleavage and cleavage of its substrate poly-ADP ribose polymerase (PARP; Fig. 3 A). Next, the Fas-induced release of cytochrome *c* and Smac/Diablo from mitochondria of tafazzin-knockdown cells was analyzed by immunostaining. It is worth mentioning that the levels of cytochrome *c* within the mitochondria were unaltered in untreated cells regardless of the CL status (Figs. 3 B and 4 C). Although in many control cells (Fig. 3 B and C, white arrows), cytochrome *c*

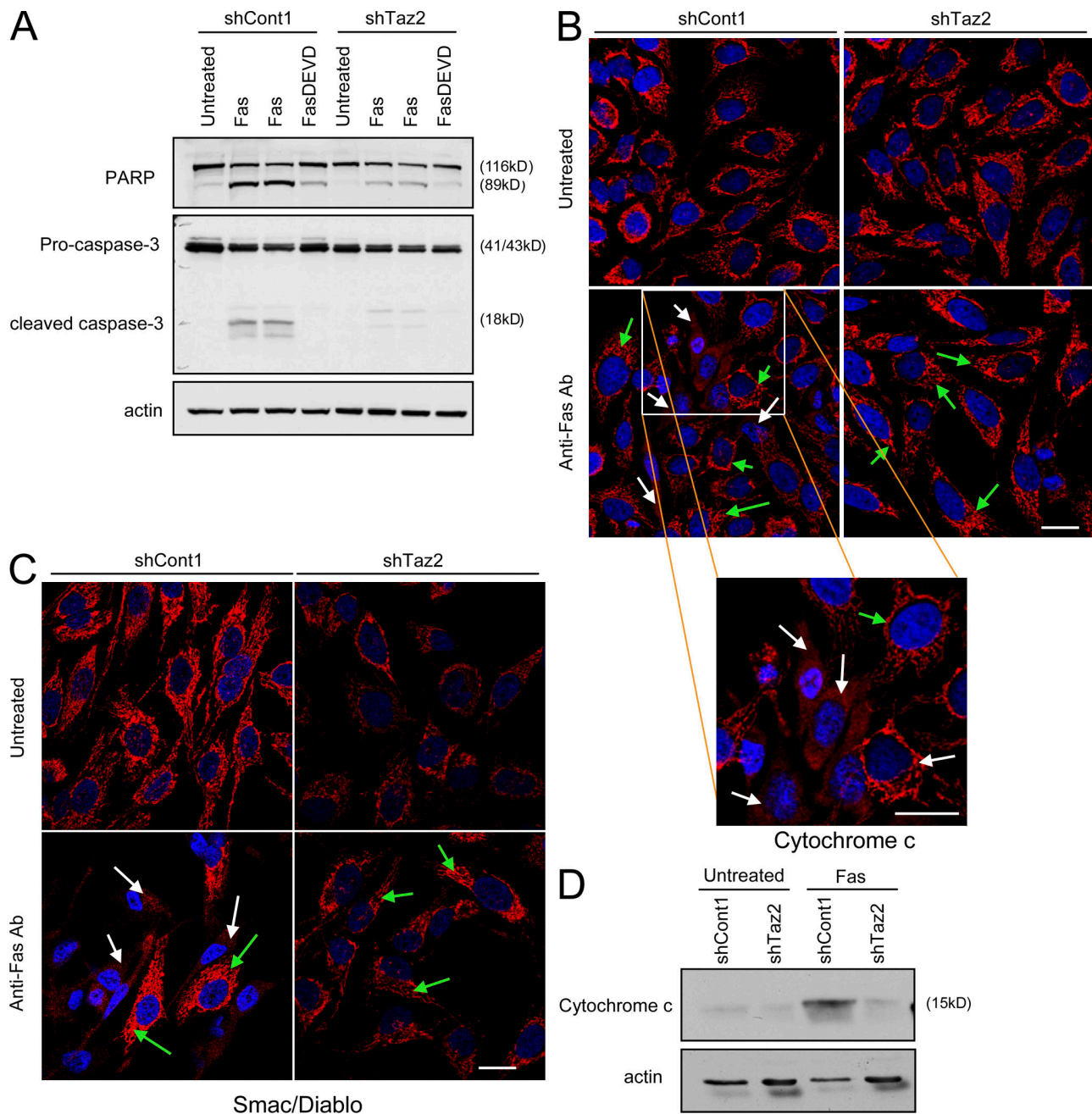


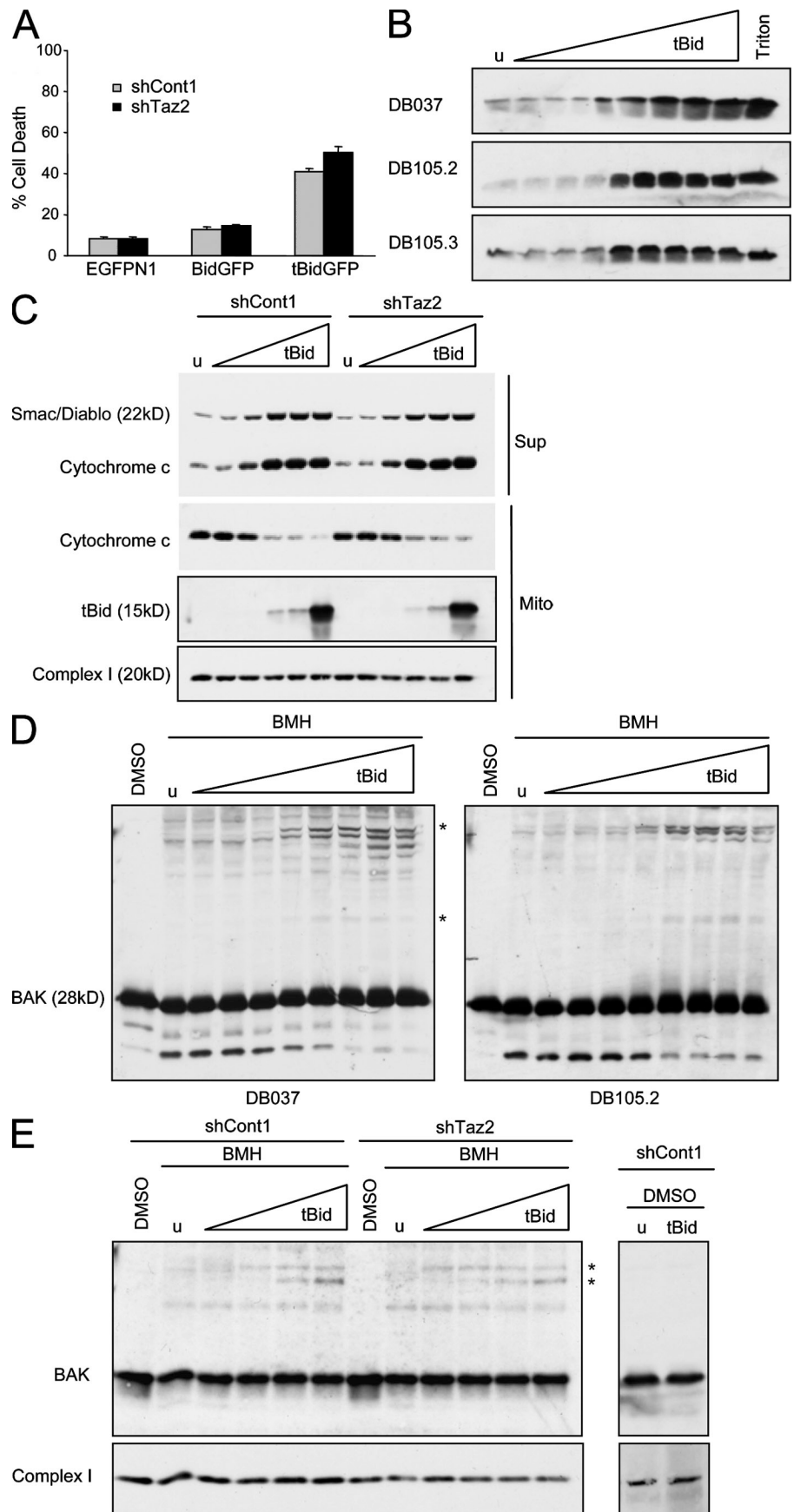
Figure 3. Tafazzin-deficient cells are defective in cytochrome *c* and Smac/Diablo release from mitochondria and in the activation of caspase-3 after Fas activation. (A) Caspase-3 activity of control (shCont1) and tafazzin-deficient HeLa cells (shTaz2) was monitored in untreated, anti-Fas antibody-treated for 14 h (Fas), and anti-Fas antibody- and DEVD-fmk-treated cells (FasDEVD). PARP and caspase-3 cleavage, both known caspase-3 targets, were analyzed by Western blotting. (B) Cytochrome *c* release from mitochondria before and after a 14-h treatment with anti-Fas antibody in the presence of DEVD-fmk was analyzed in control (shCont1) and tafazzin-knockdown (shTaz2) cells by immunostaining. The release of cytochrome *c* was evident in several cells in each microscopic field, judged by the diffusion of the protein in the cytosol and by the overall lower intensity of the immunostained protein (white arrows). Cells in which cytochrome *c* is retained in the mitochondria (punctuated staining and high intensity) are indicated by green arrows. DAPI was used to stain the nuclei. (C) Smac/Diablo release was analyzed as for cytochrome *c*. (D) Cytochrome *c* release was detected by a Western blot analysis of cytosolic fractions of the indicated cells treated as in B. Bars, 10 μ m.

and Smac/Diablo appeared in the cytosol after Fas activation, both proteins were retained in the mitochondria in all CL-deficient cells (Fig. 3, B and C). Western blot analysis of cytosolic fractions confirmed a block in cytochrome *c* release from the mitochondria of tafazzin-knockdown cells after Fas activation (Fig. 3 D). Therefore, the apoptotic block in CL-deficient cells is caused by defects in mitochondrial outer membrane permeabilization or upstream events.

tBid induces mitochondrial outer membrane permeabilization and apoptosis of CL-deficient cells

It was previously suggested that in the mitochondria-dependent step of apoptosis, CL enables tBid docking and supports Bax oligomerization on the mitochondrial outer membrane (Lutter et al., 2000; Kuwana et al., 2002). However, transient transfection with a tBid-expressing vector showed tafazzin-knockdown

Figure 4. CL-deprived mitochondria efficiently release cytochrome c and Smac/Diablo after treatment with recombinant tBid protein. (A) The indicated cells were transfected with either empty vector control (EGFPN1) or with a plasmid encoding either full-length Bid protein fused to GFP (BidGFP) or a fused tBid-GFP protein (tBidGFP). Cell death was assessed by PI exclusion in GFP-positive cells by FACS analysis. Error bars represent \pm standard deviation. (B) A cytochrome c-releasing assay of mitochondria isolated from control (DB037) or Barth syndrome-derived lymphoblastoid cells (DB105.2 and DB105.3). Mitochondria were either left untreated (u) or treated with increasing amounts of tBid (0.05, 0.1, 0.2, 0.5, 1, 5, 10, and 50 nM). Triton X-100 was used as a positive control for maximal cytochrome c release. In all cases, cytochrome c was efficiently released to the supernatant buffer when mitochondria were treated with tBid concentrations of 0.5 nM or higher. (C) Mitochondria were isolated from control-transfected (shCont1) or tafazzin knockdown (shTaz2) HeLa cells, and were either left untreated (u) or treated with increasing amounts of tBid (0.05, 0.1, 0.25, 0.5, and 5 nM). Cytochrome c and Smac/Diablo were analyzed in the supernatant (Sup) and cytochrome c, and tBid (translocated to the mitochondria) and subunit 6 of complex I (as mitochondrial loading control) were analyzed in the mitochondrial pellet (Mito). Efficient release of cytochrome c and Smac/Diablo from the mitochondria as well as the translocation of tBid to the mitochondria were identified at tBid concentrations equal to 0.1 nM or higher. (D and E) Mitochondria were isolated from control or tafazzin-deficient lymphoblastoid cells (D) or HeLa cells (E), and Bak oligomerization on the mitochondria was analyzed after treatment without (u) or with increasing amounts of tBid, as indicated in B and C. BMH (protein cross-linker) or DMSO (control solvent) were added after incubation with tBid. No higher molecular weight forms of Bak were observed in the absence of BMH, even when the maximal tBid concentration was added (E, right). Asterisks indicate multimers of the Bak protein.



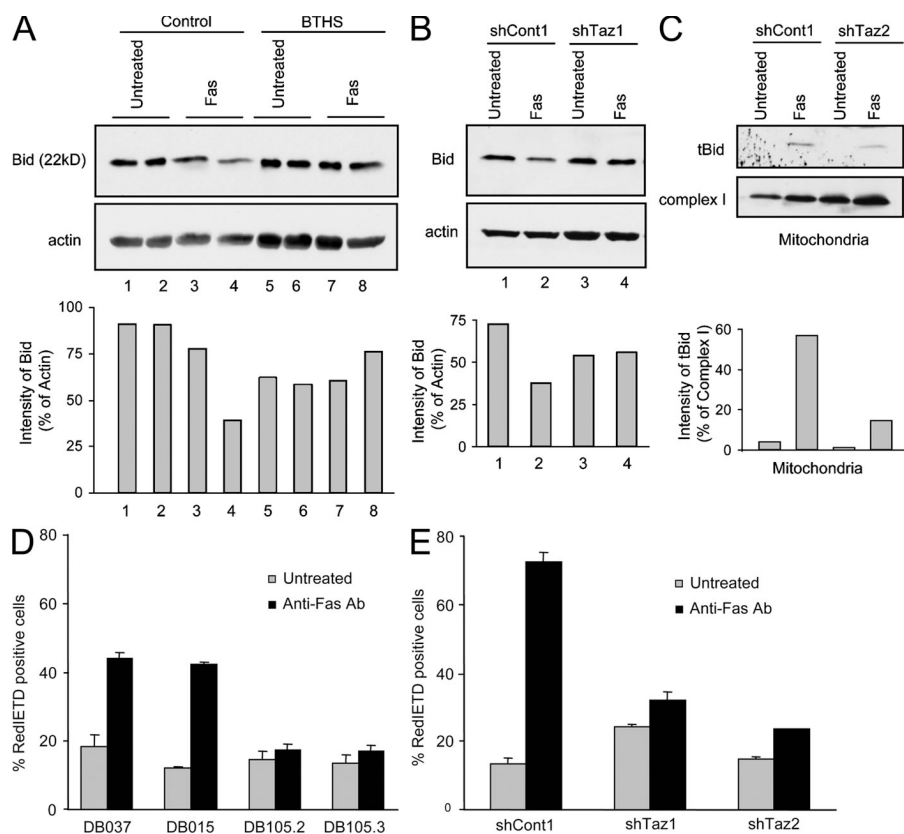


Figure 5. Caspase-8 activity is abrogated in tafazzin-deficient cells. (A) Control lymphoblastoid cells (DB037, lanes 1 and 3; DB015, lanes 2 and 4) and Barth syndrome–derived lymphoblastoid cells (DB105.2, lanes 5 and 7; DB105.3, lanes 6 and 8) were either untreated or treated with anti-Fas antibody (Fas) for 14 h. Total cell extract was analyzed by Western blotting for Bid levels. After digital scanning of the immunoblot, the intensities of Bid levels as a percentage of actin levels were plotted (bottom). (B) Control (shCont1) and tafazzin-knockdown (shTaz1) HeLa cells were either untreated or treated with anti-Fas antibody for 14 h, and analyzed as in A. (C) Mitochondria were isolated from the indicated cells treated as in B, and the tBid levels on the mitochondria were analyzed by Western blotting. Subunit 6 of complex I was used as a mitochondrial marker and loading control. After digital scanning of the immunoblot, the intensities of tBid levels as a percentage of complex I levels were plotted (bottom). (D and E) The indicated control or tafazzin-deficient cells were treated as in A and analyzed for IETDase (caspase-8–like) activity. Error bars represent \pm standard deviation.

cells to be as sensitive as control cells to tBid-induced cell death (Fig. 4 A). Isolated mitochondria from either control, Barth syndrome–derived lymphoblastoid, shCont1 HeLa, or shTaz2 HeLa cells were then incubated with increasing amounts of recombinant tBid protein, and the release of cytochrome *c* and Smac/Diablo was analyzed. In agreement with the results observed in cells, the response of CL-deficient mitochondria to tBid was comparable to control mitochondria (Fig. 4, B and C). Moreover, tBid incorporated into mitochondria (Fig. 4 C) and induced Bak oligomerization (Fig. 4, D and E) to the same extent in both tafazzin-deficient and control cells. The explanation for these surprising observations could be that the less-mature CL in tafazzin-deficient cells is sufficient for tBid interaction with mitochondria. Indeed, it has been previously demonstrated that tBid can efficiently interact with MLCL (Esposti et al., 2003; Liu et al., 2005). However, these observations clearly indicate that the block to apoptosis in tafazzin-deficient cells lies upstream to tBid activity.

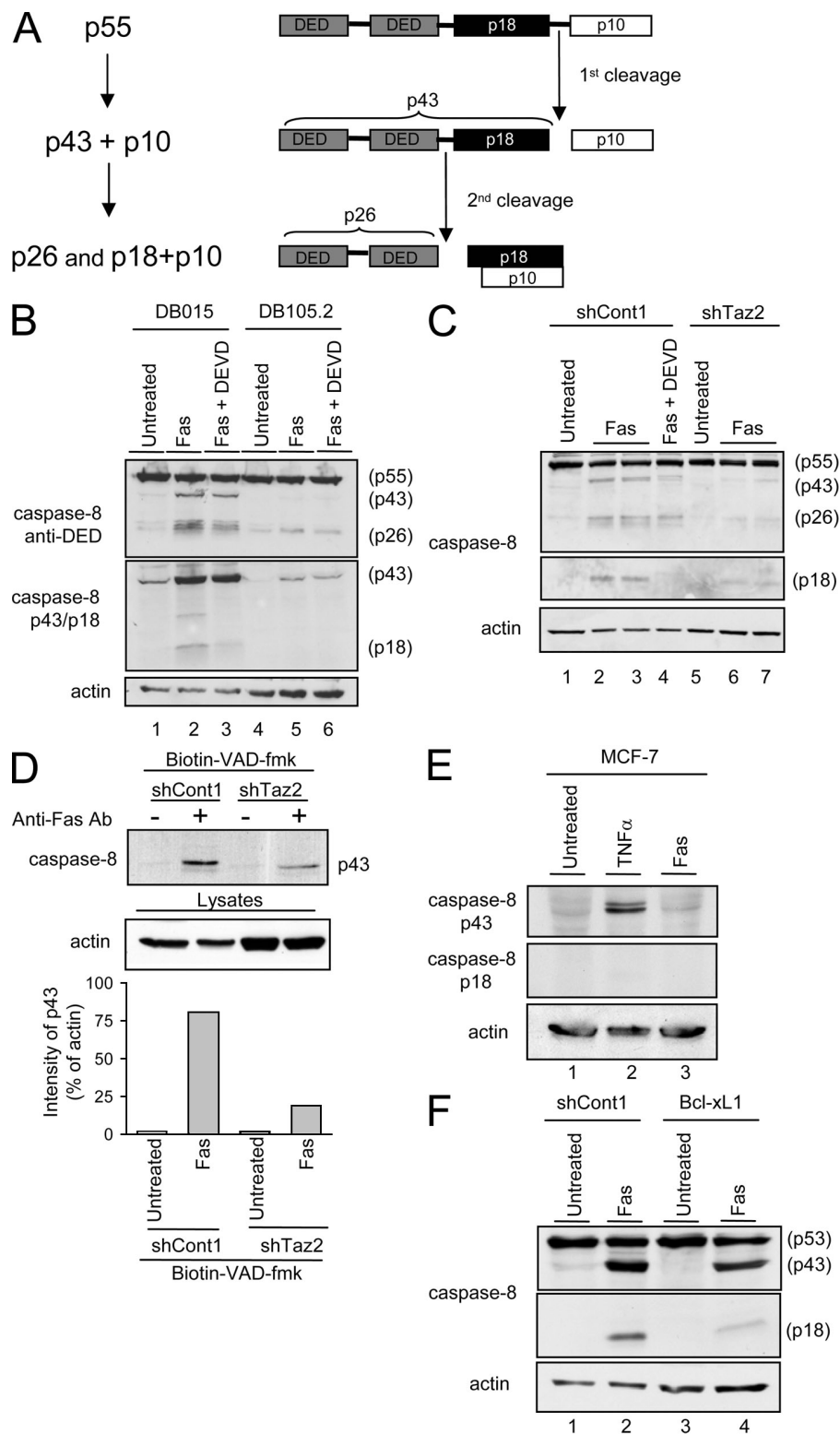
Activation of caspase-8 on the mitochondria requires CL

Bid cleavage was then analyzed in control and tafazzin-deficient cells. Because of technical difficulties in immunodetecting tBid in total cell extracts, changes in the levels of full-length Bid rather than of tBid were initially measured. Fas activation decreased the levels of full-length Bid in control but not in CL-deficient cells, which indicates a block in Bid processing (Fig. 5, A and B). To detect tBid directly, mitochondria from control and tafazzin-knockdown HeLa cells were isolated before and after Fas activation. As expected, tBid was clearly detected on mitochondria of

Fas-activated control cells, whereas on mitochondria of tafazzin-knockdown cells, tBid formation was markedly reduced (Fig. 5 C). Because Bid is cleaved by caspase-8 after Fas activation, it seemed likely that in tafazzin-deficient cells, Bid was not processed because of the inactivity of caspase-8. Therefore IETDase (caspase-8–like) activity was monitored in lymphoblastoid and HeLa cells, and was indeed found to be diminished in tafazzin-deficient cells (Fig. 5, D and E).

Caspase-8, which is an initiator caspase, is activated by induced homoproximity that leads to autoprocessing of the proenzyme to a mature, more potent form (Chen et al., 2002; Donepudi et al., 2003). Upon homodimerization, procaspase-8 (p55) is first cleaved between its two active subunits, p10 and p18, to generate the p43/p10 heterodimer (Fig. 6 A). Then, cleavage of p43 between the death effector domain (DED) and the p18 subunit produces the fully active p18–p10 form. To follow caspase-8 processing in the different cell lines, immunospecific antibodies against the autocleavage products of caspase-8 were used. As can be seen in Fig. 6 (B and C), caspase-8 autocleavage products are notably low in both Barth syndrome–derived lymphoblastoid cells (Fig. 6 B, compare lanes 2 and 5) and tafazzin knockdown HeLa cells (Fig. 6 C, compare lanes 2 and 3 with 6 and 7). To specifically analyze caspase-8 activation, biotinylated-VAD-fmk peptide (bVAD) was used. bVAD binds and inhibits active caspases, and hence is used to precipitate the first initiator caspase activated in cells after an apoptotic insult (Tu et al., 2006). bVAD precipitated high amounts of active caspase-8 (p43) from Fas-activated control HeLa cells (Fig. 6 D). However, a significant reduction in precipitated active caspase-8 was observed in tafazzin-deficient HeLa cells (Fig. 6 D). Together,

Figure 6. Caspase-8 processing is defective in tafazzin-deficient cells. (A) A schematic diagram of caspase-8 autoprocessing during Fas-mediated apoptosis. (B) Control and Barth syndrome-derived lymphoblastoid cells were treated as in Fig. 5 A and analyzed by Western blotting for caspase-8 cleavage. Two different antibodies were used: anti-DED of caspase-8 and anti-p18 domain (which also detects the cleaved p43 form). (C) Control and tafazzin-knockdown HeLa cells were treated as in Fig. 5 B and analyzed for caspase-8 cleavage as in B. (D) The different HeLa-derived clones were treated with anti-Fas antibody as indicated for 14 h. The lysates were incubated with biotin-VAD-fmk to precipitate active caspases, and active caspase-8 was detected by immunoblotting. The graph represents a densitometric analysis of the p43 immunoblot as a percentage of total actin levels. (E) MCF-7 cells were either left untreated or treated with either TNF- α together with cycloheximide (TNF- α) or anti-Fas antibody (Fas). Caspase-8 processing was assessed by the anti-p18 antibody. (F) shCont1 and Bcl-xL-expressing HeLa cells were treated as in Fig. 5 B, and caspase-8 activation was assessed by anti-DED (top) or anti-p18 (middle) antibodies.



these results strongly indicate defective caspase-8 activation in CL-deficient cells.

Even though caspase-8 is an important initiator caspase in the Fas signaling response, it was necessary to test whether the decrease in caspase-8 activity in tafazzin-deficient cells results from a decrease in the amplification loop signaling from caspase-3 or caspase-6 back to caspase-8 (Slee et al., 1999). To this

end, control lymphoblastoid cells were treated with anti-Fas antibody in the presence of the effector-caspase inhibitor DEVD-fmk. No change in the early processing of procaspase-8 to its product p43 was observed (Fig. 6 B, top, compare lanes 2 and 3). However, DEVD-fmk significantly blocked the processing of p43 into its fully mature p18-p10 form (Fig. 6 B, middle, compare lanes 2 and 3). Similar results were obtained in control HeLa

cells (Fig. 6 C; compare lanes 2 and 3 with lane 4). Interestingly, a block in p18 but not in p43 formation was also observed in Fas-activated cells treated with the pan-caspase inhibitor zVAD-fmk (unpublished data). These results indicate that a caspase-dependent amplification loop is not required for early processing of caspase-8 to p43 and also show that the first cleaving step of caspase-8, induced by its dimerization, is not inhibited by zVAD-fmk. To bypass the use of pharmacological inhibition of caspases, MCF7 cells, which carry an inactive mutant form of caspase-3, were analyzed. MCF7 cells do not express Fas and therefore did not respond to anti-Fas antibody, but when treated with TNF- α , even though they were protected from cell death, formation of p43 but not of p18 was clearly observed (Fig. 6 E). In addition, similar results were obtained in HeLa cells in which mitochondria-dependent apoptosis upstream of caspase-3 activity was blocked by overexpression of Bcl-xL (Fig. 6 F). Put together, these results indicate that although caspase-3 amplification (downstream to the mitochondria) is required for full activation of caspase-8, it is not required for the early stage of caspase-8 processing. Because in CL-deficient cells the block in caspase-8 activation is seen in the initial processing of procaspase-8 into p43 (Fig. 6, B and C), the CL-dependent apoptotic step is most likely independent of caspase-3 and lies either at or upstream of the mitochondrial steps of apoptosis.

It was previously found that caspase-8 interacts with mitochondria under both physiological (Stegh et al., 2000) and apoptotic conditions (Stegh et al., 2002; Chandra et al., 2004). Seeing that a mitochondrial lipid affected caspase-8 activity in type II apoptotic signaling, we investigated whether CL is required for caspase-8 interaction and activation on the mitochondria. Cytosolic and mitochondrial fractions of control, tafazzin-deficient lymphoblastoid and HeLa cells were isolated before and after Fas activation and analyzed for caspase-8 levels. Although after Fas-activation, mitochondria of control cells displayed cleaved caspase-8 products, including p43 and p18 (Fig. 7, A and B, lane 6), on mitochondria of CL-deficient cells, these products were significantly reduced (Fig. 7, A and B, compare lanes 6 and 8). The activity of caspase-8 on isolated mitochondria was measured using benzyloxycarbonyl-Leu-Glu-Thr-Asp (zLETD)-aminoluciferin as a substrate. LETDase activity was much higher in mitochondria isolated from Fas-activated control HeLa cells compared with the tafazzin-deficient HeLa cells (Fig. 7 C), which indicates a defect in caspase-8 processing in tafazzin-deficient mitochondria. This suggests that mitochondria are a required location for full activity of caspase-8. Importantly, the p43 and p18 mitochondria-associated products, and to a lesser extent procaspase-8 or the DED domain, were resistant to alkaline wash (Fig. 7 D). This indicates the strong insertion of the p18-exposed isoforms of caspase-8 into the mitochondrial membrane. To determine if caspase-8 completely inserts into the mitochondria, mitochondria were isolated from HeLa cells that had been transiently transfected with the partially active caspase-8 mutant C360S fused to GFP in the presence of zVAD-fmk (for more details on this mutant, see Fig. 8 C). The isolated mitochondria were incubated with increasing concentrations of trypsin. The data indicated that C360S-GFP and p43-C360S were sensitive to trypsin treatment (Fig. 7 E) and

suggested that caspase-8 is only partially inserted into the mitochondrial outer membrane, where it mostly faces the cytosol.

The question remained as to how caspase-8 interacts with CL on the mitochondria. CL accumulates at the contact sites between the inner and outer mitochondrial membranes, where it facilitates tBid translocation to the mitochondria (Ardail et al., 1990; Hovius et al., 1990; Simbeni et al., 1991; Lutter et al., 2001; Kim et al., 2004). One possibility was that the enzyme translocates to the mitochondria together with its known substrate, Bid. However, in Bid knockdown cells, caspase-8 translocation to the mitochondria after Fas activation was unaffected (Fig. 7 F). Caspase-8 interaction with the mitochondria may be mediated by other proteins (Stegh et al., 2002). However, as was described for tBid, it is plausible that in addition to formation of protein-protein interactions, caspase-8 also interacts directly with the CL, where CL facilitates and strengthens the protein-membrane association. To test this possibility, liposomes containing the lipid composition of the mitochondrial contact sites were incubated with *in vitro*-translated caspase-8. Liposomes in which CL was replaced with PC and phosphatidylethanolamine (PE) were used to investigate the exclusive requirement for CL in caspase-8 binding. Analysis of the precipitated liposomes showed no significant changes in p55 pro-caspase-8 interaction with CL-containing as compared with CL-deficient liposomes (Fig. 7 G). These results are in line with the results observed in isolated mitochondria (Fig. 7 B). However, as with mitochondria, the levels of p43 autoprocessed form were significantly reduced in CL-deficient as compared with CL-containing liposomes (Fig. 7 G). Importantly, there is a significant enrichment of the p43-processed form of caspase-8 in CL-containing liposomes as compared with the input (*in vitro*-translated p55). This may be either due to the activation by proximity of pro-caspase-8 on the liposome or because of the fact that once cleaved in the buffer, p43 has an increased affinity to the membrane. The stability of the interaction between *in vitro* translated caspase-8 and CL-containing liposomes was assessed after washing the precipitated liposomes in 0.1 M Na₂CO₃, pH 11.5, or in 1 M NaCl. A small fraction of caspase-8 was extractable, but the majority remained associated with the liposomes (Fig. 7 H). Altogether, these results suggested a stable insertion of caspase-8 into the liposomes, which are mediated by hydrophobic interactions with CL. This however, does not rule out the possibilities that electrostatic interactions with CL and/or protein-protein interactions also facilitate caspase-8 interaction with the mitochondria.

Importantly, after Fas activation in both tafazzin-knockdown and control cells, the cytosolic procaspase-8 was fully cleaved into its early mature form (p43; Fig. 7 B, lanes 2 and 4). This indicates that in the cytosol, the initiating process of caspase-8 cleavage (on the DISC) is unaffected in tafazzin-knockdown cells, and that the major defects in these cells lie in the steps of docking and activation of caspase-8 on the mitochondria. In type II cells, the activation of caspase-8 on the DISC is limited, hence the need for a mitochondria-mediated amplification step. To test whether loss of CL hinders only the mitochondria-dependent (but not mitochondria-independent) apoptotic steps, a caspase-8-GFP fusion protein was transiently expressed in HeLa cells. This fusion protein can oligomerize and self-activate in

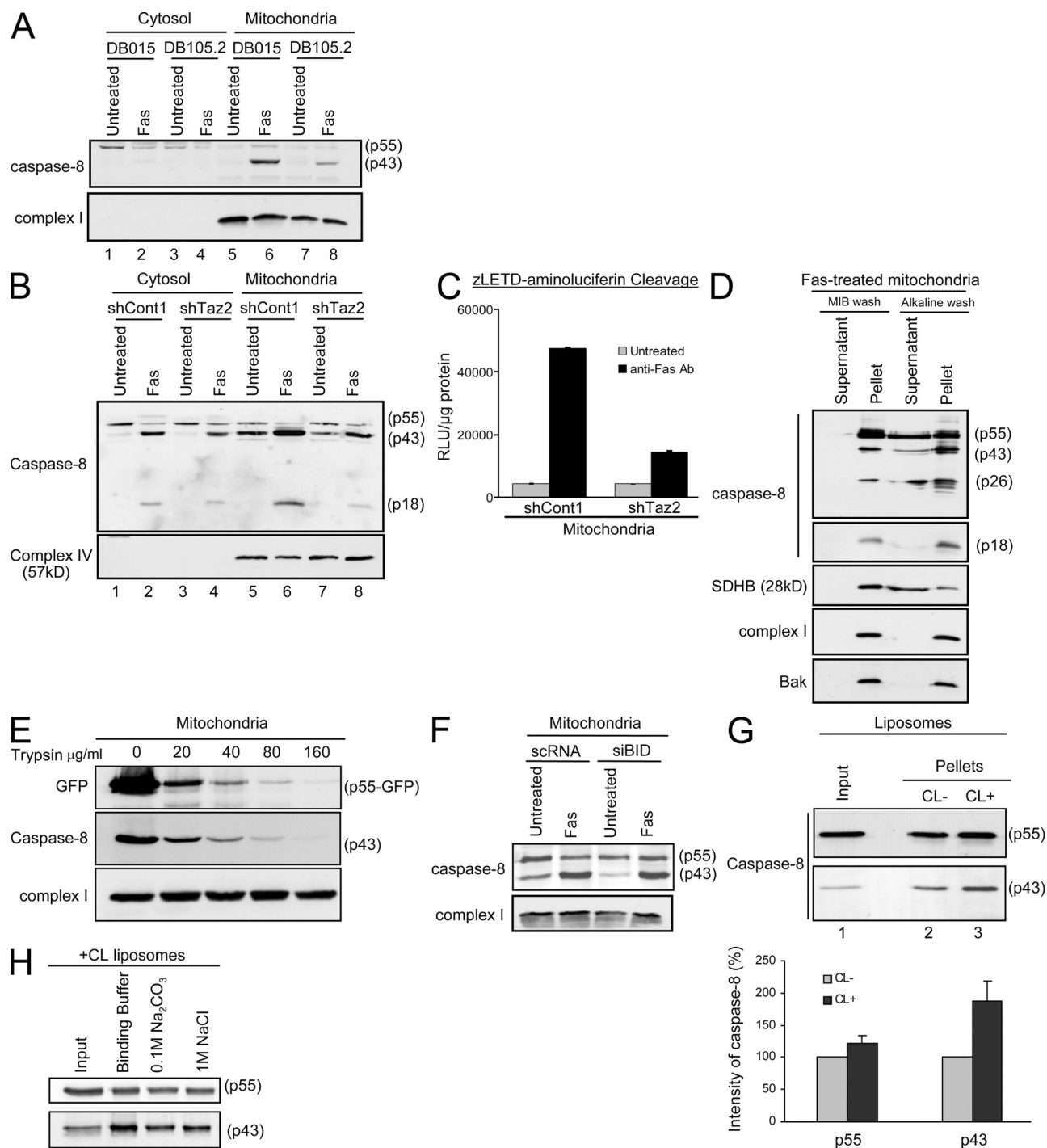


Figure 7. Caspase-8 translocation to the mitochondria is blocked in CL-deficient cells. (A) Control (DB015) and Barth syndrome–derived (DB105.2) lymphoblastoid cells were either left untreated or treated with anti-Fas antibody for 24 h. Cytosolic and mitochondria-enriched fractions were isolated, and caspase-8 localization and autoprocessing was analyzed by Western blotting using the anti-DED antibody. Subunit 6 of complex I was used as a mitochondrial marker and loading control. (B) The different HeLa-derived clones were treated as indicated, and cells were fractionated to cytosolic and mitochondria-enriched fractions. The cleaved products of caspase-8 were analyzed with the anti-p18 antibody. Subunit 4 of complex IV was used as a mitochondrial marker and loading control. (C) Mitochondria were isolated from HeLa cells treated with anti-Fas antibody as indicated. The cleavage of zLETD-aminoluciferin was used to assess caspase-8 activity on the mitochondria. The graph shows the relative levels of emitted signal from the experiment displayed in arbitrary units of luminescence (RLU) per microgram of protein. Error bars represent \pm standard deviation. (D) Mitochondria were isolated from HeLa cells treated with anti-Fas antibody and either washed with MIB only or with alkaline MIB. The pellet and supernatant of each wash were analyzed for caspase-8 (DED and p18 domains). The different cleaved products of caspase-8 are indicated on the right. Succinate dehydrogenase complex subunit B (SDHB) was used as a control for loosely attached proteins, and complex I and Bak were used as control for membrane-inserted proteins. (E) Mitochondria were isolated from HeLa cells transfected with caspase-8–C360S–GFP in the presence of zVAD-fmk. Isolated mitochondria were subjected to trypsin digestion at the indicated concentrations. Mitochondrial pellets were analyzed by immunoblotting. (F) HeLa cells were transiently transfected with either control siRNA (scRNA) or siRNA targeting Bid (siBid), as in Fig. S2 (available at <http://www.jcb.org/cgi/content/full/jcb.200803129/DC1>). 48 h later, cells were either left untreated or treated with anti-Fas antibody for 14 h. Mitochondria were then isolated, and caspase-8 localization and autoprocessing was

the cytosol in the absence of Fas signaling, inducing a type I-like response (unpublished data). When overexpressed in HeLa cells, caspase-8-GFP induced cell death, which could not be blocked by Bcl-xL (Fig. 8, A and B). Because the tafazzin knockdown cells are GFP positive (see Materials and methods for details), cell death after caspase-8-GFP transfection was assessed in these cells by PARP cleavage, an indicator for caspase-3 activation. As can be seen in Fig. 8 B, overexpressing caspase-8-GFP induced comparable cell death in both control and tafazzin knockdown cells. These results indicate that like Bcl-xL overexpression, tafazzin knockdown provides protection from the mitochondria-dependent but not from the mitochondria-independent apoptotic steps.

The point mutation C360S within the catalytic domain of caspase-8 reduces its activity but preserves its autoprocessing into p43 (Chang et al., 2003). When transfected into HeLa cells, the C360S-GFP was partially processed into p43 but not into p18 (Fig. 8 C). As discussed earlier, this autoprocessing can occur even in the presence of zVAD-fmk, which in the following experiment was used to prevent cell death and further processing of the mutated enzyme by other caspases (as part of the amplification loop). To investigate whether the exogenous caspase-8 fusion protein translocates into the mitochondria in a CL-dependent manner, shCont1 and shTaz2 were transiently transfected with C360S-m-Cherry (a fusion protein of monomeric red fluorescent protein and the C360S point mutant). This was done to avoid using green fluorescence in these GFP-positive cells. Under these conditions, when shCont1 cells were transfected with C360S-m-Cherry, the vast majority of transfected cells (>70%) showed mitochondrial localization of the fusion protein (Fig. 8 D, top). Mitochondria were visualized in this experiment by immunostaining for TOM20. It is important to indicate that even after autoprocessing, the C-terminally tagged m-Cherry, which is fused to the cleaved p10, would colocalize with p43 on the mitochondria as a heterodimer. In contrast, when the C360S-m-Cherry mutant was expressed in tafazzin knockdown cells, the majority of cells showed a diffused cytosolic pattern (Fig. 8 D, bottom). The BH3-only protein tBid has been shown to interact exclusively with liposomes that contain CL (Lutter et al., 2000), and electron tomogram studies showed that tBid interacts with the contact sites of mitochondrial membranes, an area rich in CL (Lutter et al., 2001). Colocalization between tBid and caspase-8 would therefore suggest that caspase-8 also localizes to CL-enriched domains of the mitochondria. Control HeLa cells were cotransfected with tBid-GFP and C360S-m-Cherry in the presence of zVAD-fmk and imaged by confocal microscopy. Colocalization was observed between tBid and caspase-8 (Fig. 8 E). These results provide further support for the observation that caspase-8 interaction with the mitochondria is CL dependent, and suggest that, like tBid, caspase-8 also localizes to CL-rich domains on the mitochondrial contact sites.

Finally, it was investigated whether caspase-8 translocation to the mitochondria is required for its activation. As mentioned before, initiator caspases are activated via induced proximity, and it seemed possible that after its insertion into the CL-enriched mitochondrial membrane, caspase-8 dimerizes and autoprocesses to become activated. Therefore, caspase-8 oligomerization on the mitochondrial membrane after Fas activation was examined. Isolated mitochondria from Fas-activated shCont1 cells were treated with the cross-linker *Bis*-maleimidohexane (BMH). p43 monomers were noted in control (DMSO) lanes but were absent in the BMH-treated lanes. However, higher molecular weight oligomers were present in the BMH-treated mitochondria lanes (Fig. 9). In particular, ~53-kD and ~80-kD forms were observed, which indicates that upon mitochondrial translocation, caspase-8 forms a p43/p10 homo-heterodimer (Fig. 9). This tetrameric form of caspase-8 is known to be active (though not to its full capacity) and can explain the caspase-8 activity observed on isolated mitochondria (Fig. 7 C). However, this form may be an intermediate on its way to be processed to form the p18-p10 fully active complex. The fate of this caspase-8 form is still unclear and is under investigation. Interestingly, however, higher molecular weight forms were also observed, indicating that caspase-8 may further oligomerize on the mitochondria or that it is associated with other mitochondrial proteins. It is of note that once cleaved from p43, the DED domain (p26) on its own is no longer affected by the cross-linker and is probably released from the oligomer when caspase-8 is further processed to its fully active p18-p10 form. To summarize: the localization, oligomerization, and cleavage of caspase-8 on the mitochondria after Fas activation, and the deficits in these processes in CL-deficient cells, strongly indicates that CL provides an activating platform for caspase-8 on the mitochondria after Fas stimulation.

Discussion

Several studies have previously shown that CL is involved in the mitochondria-dependent steps of apoptosis (Lutter et al., 2000; Kuwana et al., 2002; Liu et al., 2004; Kim et al., 2004; Gonzalez et al., 2005a,b; Kagan et al., 2005). However, until recently, the role of CL in apoptosis was not addressed directly in cells. After the identification of human CL synthase, the role of CL in apoptosis was studied in a mammalian cell model in which CL synthase was knocked down. However, these cells displayed severe bioenergetic defects that led to accelerated cell death with necrotic features (Choi et al., 2007). In this work, the role of CL was investigated using novel cell models of Barth syndrome patient-derived cells and tafazzin knockdown HeLa cells, which contain significantly reduced amounts of mature CL. These CL-deprived cells are resistant to Fas-induced apoptosis. However, their mitochondria are fully capable of undergoing

detected by Western blotting using the anti-DED antibodies. Subunit 6 of complex I was used as loading control. (G) Liposomes were prepared with or without CL and incubated for 30 min at 37°C with *in vitro* translated procaspase-8 protein. Liposomes were then precipitated and washed, and caspase-8 binding to the lipid membrane was analyzed by Western blotting. The input lane represents 20% of the sample after incubation with caspase-8 but before precipitation. The graph shows the relative intensity of the different caspase-8 forms on liposomes with or without CL, and is the mean and standard deviation of three independent experiments. Error bars represent \pm standard deviation. (H) CL-containing liposomes were incubated with caspase-8 and either washed once in binding buffer, or in alkalic (0.1 M Na₂CO₃, pH 11.5) or high-salt (1 M NaCl) buffers. After precipitation of liposomes, caspase-8 levels were assessed by immunoblotting. The input lane is as in G.

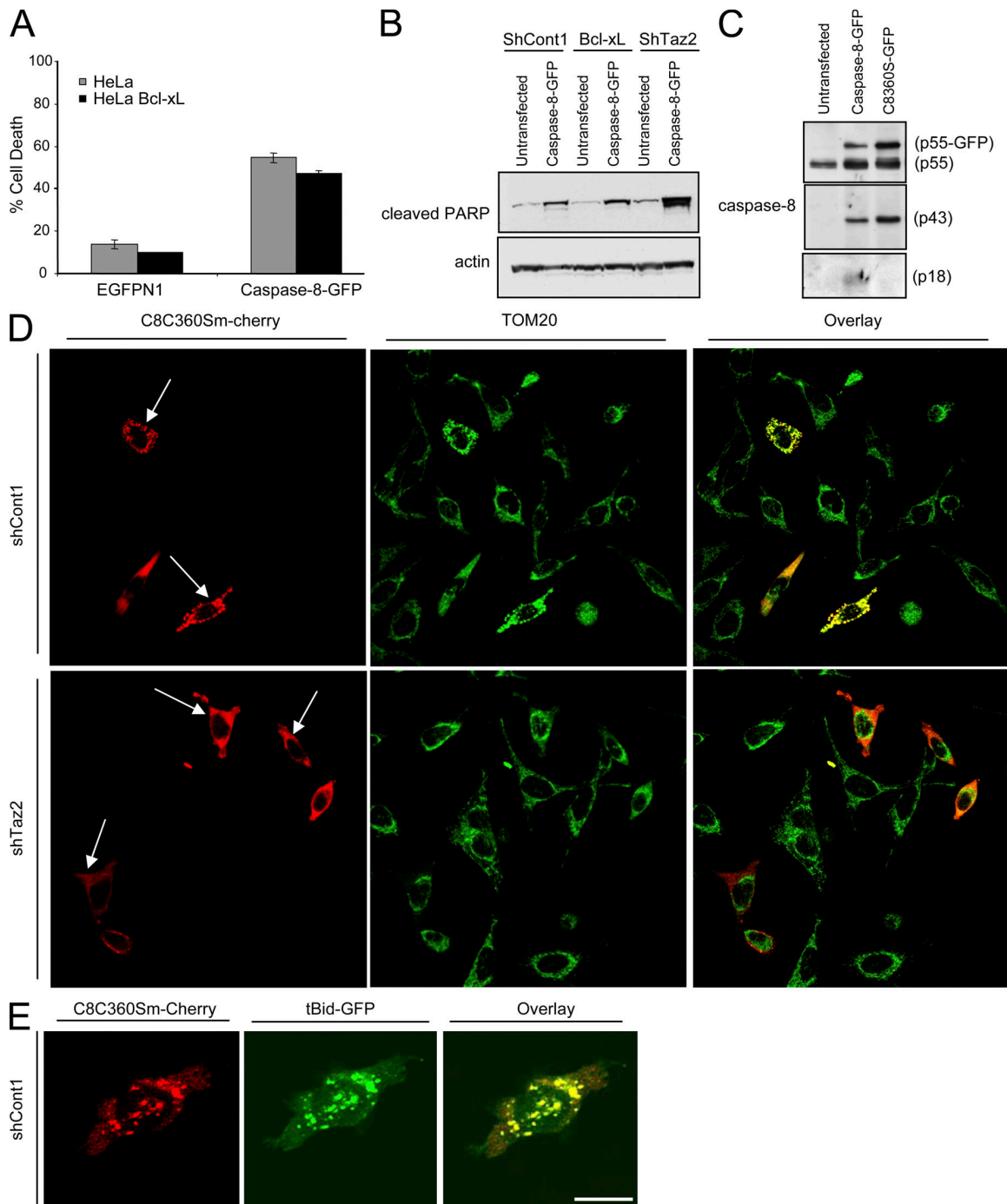


Figure 8. Caspase-8 C360S colocalizes with tBid on the mitochondria. (A) Parental or Bcl-xL-overexpressing HeLa cells were transfected with either empty vector (EGFPN1) or with a plasmid encoding the caspase-8-GFP fusion protein. Green cells were analyzed by FACS for viability using PI exclusion. Error bars represent \pm standard deviation. (B) The indicated HeLa cells were either left untransfected or transfected with the caspase-8-GFP fusion protein. 24 h later, cells were lysed and analyzed for PARP cleavage (using anti-cleaved PARP antibody) as an indicator of cell death. (C) HeLa cells were either left untransfected or transfected with the indicated caspase-8-GFP protein. The presence of the different caspase-8 processed forms was detected using different anti-caspase-8 antibodies. (D) Control and tafazzin-knockdown cells were transfected with caspase-8 C360S mutant fused to m-Cherry (C8C360S-m-Cherry), and 24 h later, cells were fixed and stained for TOM20 as a mitochondrial marker. Alexa 647-conjugated secondary antibody was used for a far-red fluorescence detection of the mitochondria (artificially presented in green). (E) Control HeLa cells were transfected with C8C360S-m-Cherry and tBid-GFP in the presence of zVAD-fmk, and 16 h later, cells were fixed and analyzed by confocal microscopy. Bars, 10 μ m.

the steps required for apoptosis in response to tBid, such as Bak oligomerization and mitochondrial outer membrane permeabilization. This prompted investigation of the impaired apoptotic process, focusing on the pathway connecting Fas to the mitochondria, and revealing that the major block is at the level of

caspase-8 activation. We propose that CL is required for the processing of caspase-8 on mitochondria, and that the interaction with CL is crucial for caspase-8 activation in type II cells.

The activation of initiator caspases requires an activating platform that enables their association with each other. Such

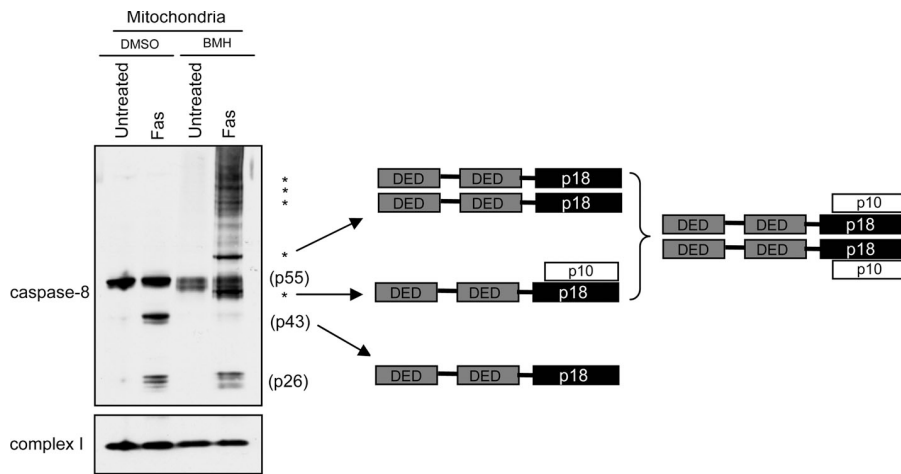


Figure 9. Caspase-8 oligomerizes on the mitochondrial outer membrane. Control HeLa cells (shCont1) were either left untreated or treated with anti-Fas antibody for 14 h, and mitochondria were isolated in the presence (BMH) or absence (DMSO) of a protein cross-linker. Subunit 6 of complex I was used as loading control. The different proposed caspase-8 oligomers are indicated on the right. Asterisks indicate higher molecular weight multimers of caspase-8.

triggering complexes include the DISC for caspase-8 and -10 (Kischkel et al., 1995), the apoptosome for caspase-9 (Zou et al., 1999), the PIDDosome for caspase-2 (Tinel and Tschoop, 2004), and the inflammasome for caspase 1 and 5 (Martinon et al., 2002). In this work, CL was identified as a potential new mitochondria-associated triggering platform required for caspase-8 translocation, oligomerization, and activation after Fas signaling in type II cells. Our data show that once the first cleavage of procaspase-8 occurs, the p43/p10 heteromer product inserts into the mitochondrial membrane, where it further oligomerizes and may potentially undergo cleavage to form a mitochondria-associated p18–p10 active complex. Though CL is mostly found in the mitochondrial inner membrane, several works have demonstrated an enrichment of CL in the contact sites between the inner and the outer mitochondrial membranes (Ardail et al., 1990; Hovius et al., 1990; Simbeni et al., 1991; Lutter et al., 2001; Kim et al., 2004). At the contact sites, CL mediates the binding of tBid to the mitochondrial outer membrane (Lutter et al., 2001). Therefore, it is likely that caspase-8 binding to the mitochondria is regulated in a similar way. It remains to be determined whether other proteins, such as BAR and FLASH, which were shown to mediate caspase-8 translocation to the mitochondria (Zhang et al., 2000; Milovic-Holm et al., 2007), play an auxiliary role in these processes.

In this paper, the role of CL in apoptosis was studied in cells after Fas activation. However, caspase-8 also operates in response to other death signals. Caspase-8 prevents metastasis formation from primary tumors (Stupack et al., 2006). It will be interesting to learn whether mitochondria in general and CL in particular are required for activating caspase-8 under these conditions, and whether CL levels are altered during advanced tumor development. A decrease in tafazzin expression levels has been reported in B cell lymphoma and breast carcinoma, which suggests that tafazzin loss may contribute to tumor progression (Wilson et al., 2002; Kobayashi et al., 2003). To date, Barth syndrome has not been associated with apoptotic defects or cancers. However, most cells in vivo are type I, and the mitochondrial amplification steps are only required in cells in which the DISC has been compromised, as is the case in many epithelial cancer cells (Shell et al., 2007). In addition, the early mortality age of Barth syndrome patients may explain the absence of increased cancer incidents. Importantly, however, Barth syndrome is often characterized by a developmental defect of noncom-

paction of the left ventricular myocardium (Bleyl et al., 1997), and a similar defect was observed in mice deficient in caspase-8 (Varfolomeev et al., 1998). Therefore, it is possible that the developmental abnormalities associated with Barth syndrome are due, at least partially, to inactivation of caspase-8. The role of mitochondria-associated caspase-8 in several in vivo processes should be further investigated.

Materials and methods

Plasmids and expression vectors

To generate the pEGFP/Taz expression vector, human *tafazzin* cDNA was amplified by PCR and inserted, in-frame, into the HindIII and SalI sites of pEGFPN1. The *tafazzin* targeted siRNA sequence (GGGAAAGTGAACATGAGTTT) was used to generate a short hairpin double-stranded DNA (dsDNA) oligonucleotide, which was then cloned into pSUPER/RetroGFPNeo (Oligoengine) to generate the pSUPER/shTaz vector. The nonspecific short hairpin dsDNA oligonucleotide was ligated into pSUPERGFPNeo (Oligoengine) to generate the pSUPER/shCont vector. To generate an siRNA-resistant *tafazzin* cDNA clone (pcDNA3/Taz_{mut}), the human *tafazzin* cDNA was cloned into pcDNA3, and the siRNA recognition sequence was mutated at the third position of the 182, 183, and 184 codons to conserve the amino acid sequence while protecting the mutated transcript from the siRNA effect.

Cells culture and transfection

The lymphoblastoid cells lines were generated from two unrelated Barth syndrome patients (DB105.2 and DB105.3) or two different controls (DB037 and DB015.2), and were a gift from R. Kelley (Johns Hopkins University School of Medicine, Baltimore, MD). DB105.2 and DB105.3 express tafazzin containing a single point mutation at G197E or I209D, respectively, which inactivates the protein. Lymphoblasts were immortalized ex vivo by Epstein-Barr virus infection. These cells were cultured in RPMI 1640 supplemented with 10% FCS, 2 mM L-glutamine, penicillin, and streptomycin. The cervical carcinoma HeLa cell lines were cultured in DME supplemented with 10% FCS and L-glutamine. Transfection of HeLa cells was performed using Lipofectamine 2000 (Invitrogen). Bcl-xL, shTaz, and shCont stable HeLa cell lines were generated by transfection with pcDNA3/Bcl-xL, pSUPER/shTaz, or pSUPER/shCont, respectively, and selected in G418. The revertant shTaz1R cell line was generated by cotransfecting shTaz1 HeLa cells with plpC vector (for the puromycin resistance gene), and pcDNA3/Taz_{mut} and stable clones were selected in puromycin.

For siRNA transfection, unless otherwise stated, HeLa cells were transfected with 50 nM of the indicated siRNA, and the efficiency of gene silencing was validated by Western blotting 48 h after transfection. The sequence targeted by siBid and siTaz were GAAGACATCATCCGGAATATT and GGGAAAGTGAACATGAGTTT, respectively. A nontargeting siRNA pool (Thermo Fisher Scientific) was used as control.

Lipid analysis

Lipid analysis was performed as described previously (Valianpour et al., 2002). Cells were sonicated for 20 s in PBS, and phospholipids were

extracted from the equivalent of 1 mg of protein of the homogenates as follows: after the addition of 3 ml of 1:1 chloroform/methanol (vol/vol), the internal standards (0.4 nmol of tetramyristoyl-CL and 0.16 nmol of dimyristoyl-phosphatidylglycerol; Avanti Polar Lipids) were added. This mixture was shaken vigorously and placed on ice for 15 min, after which it was centrifuged at 1,000 g for 10 min. The supernatant was transferred to new tubes, and the protein pellet was reextracted with 3 ml of 2:1 chloroform/methanol (vol/vol). The combined organic layers were evaporated under nitrogen at 45°C. The residue was dissolved in 150 μ l chloroform/methanol/water (50:45:5 vol/vol/vol) containing 0.01% NH_4OH , and 10 μ l of the solution was injected into the HPLC mass spectrometry system (Thermo Electron Corporation). The column temperature was maintained at 25°C. The lipid extract was injected onto a 2.1 \times 250 mm silica column with 5- μ m particle diameter (Merck). The phospholipids were separated from interfering compounds by a linear gradient between solution B (97:3 chloroform/methanol, vol/vol) and solution A (85:15 methanol/water, vol/vol). Solution A and B contained 0.1 ml and 0.01 ml of 25% (vol/vol) aqueous ammonia per liter of eluent, respectively. The gradient (0.3 ml/min) was as follows: 0–10 min, 20% A to 100% A; 10–12 min, 100% A; 12–12.1 min, 100% A to 0% A; and 12.1–17 min, equilibration with 0% A. All gradient steps were linear, and the total analysis time, including the equilibration, was 17 min. A splitter between the HPLC column and the mass spectrometer was used, and 75 μ l/min eluent was introduced into the mass spectrometer. A TSQ Quantum AM (Thermo Fisher Scientific) was used in the negative electrospray ionization mode. Nitrogen was used as nebulizing gas. The source collision-induced dissociation collision energy was set at 10 V, the spray voltage used was 3,600 V, and the capillary temperature was 300°C. Mass spectra of CL and MLCL molecular species were obtained by continuous scanning from m/z 400 to m/z 1,000 with a scan time of 2 s. The spectra of CL and MLCL species were acquired during their corresponding retention time in the HPLC elution profile. The CL internal standard was set at 100% in each spectrum.

Induction and assessment of cell death

Cells were treated with the optimal concentrations (0.3 μ g/ml for lymphoblastoid cells or 0.5 μ g/ml for HeLa cells) of an CH11 anti-Fas antibody clone (Millipore) or with the indicated amounts of etoposide or cisplatin. Cells were stained with PI (Invitrogen) alone or in combination with FITC-tagged Annexin V (BD). Cell death was quantified by FACS (BD).

Caspase activities were monitored using the caspase-3 and caspase-8 detection kits (EMD) according to the manufacturer's instructions, and analyzed by FACS. Alternatively, isolated mitochondria were incubated for 1 h at room temperature at a 1:1 dilution with caspase-Glo 8 reagent (Promega). The relative light unit (RLU) produced by caspase-8 cleavage of zLETD-aminoluciferin was recorded using GLOMAX software on a microplate luminometer (Veritas; Turner Biosystems).

For precipitation of active caspase-8, shCon1 and shTaz2 HeLa cells were treated with anti-Fas antibody for 16 h. After treatment, cells were lysed in a solubilization buffer supplemented with protease inhibitors and bVADfmk (EMD). Active caspase-8 was precipitated for 6 h at 4°C using streptavidin-agarose (EMD) and analyzed by immunoblotting.

For immunostaining of cytochrome c and Smac/Diablo, HeLa cells were seeded on coverslips at 2×10^5 cells/ml and treated with anti-Fas antibody in the presence of 20 μ M DEVD-fmk. 12 h after treatment, cells were fixed in 3.7% paraformaldehyde and then permeabilized in PBS/0.2% Triton X-100 and blocked in 10% FCS for 1 h. Samples were stained using anti-cytochrome c antibody (BD) or anti-Smac/Diablo antibody (BD), and then incubated with cyanine 3-conjugated anti-mouse IgG (Jackson Immuno-Research Laboratories). The coverslips were finally mounted in medium containing DAPI (Vectashield; Vector Laboratories). Samples were analyzed under a confocal microscope (SP2; Leica).

Immunofluorescence microscopy

In general, cells were grown in 6-well plates on coverslips. Cells were washed with PBS and fixed in 4% PFA for 20 min at RT. When appropriate cells, were permeabilized in 0.2% Triton X-100 in PBS, blocked with 5% BSA, and incubated overnight in anti-TOM20 (Santa Cruz Biotechnology, Inc.). Coverslips were washed and incubated in anti-rabbit IgG conjugated to Alexa 647 (Invitrogen) for 1 h and then mounted in immunofluorescence mounting medium (Vectashield; Vector Laboratories). Specimens were analyzed at room temperature using a confocal microscope (SP2 DMIRBE laser scanning confocal with SP2 software) equipped with a 63 \times /1.32 NA ph3 oil HCX Plan Apo lens (all from Leica).

Immunoblot analysis

Antibodies used for immunoblot analyses were: anti- β -actin (Sigma-Aldrich), anti-Bak (Millipore), anti-Bcl-xL serum (a gift from C. Thompson,

University of Pennsylvania, Philadelphia, PA), anti-human Bid (Cell Signaling Technology), anti-mouse Bid (Santa Cruz Biotechnology, Inc.), anti-caspase-3 (Cell Signaling Technology), anti-caspase-8 p43/p18 domain (Cell Signaling Technology), anti-caspase-8 DED domain (BD), anti-cytochrome c (7H8.2C12; BD), anti-complex I (NADH dehydrogenase subunit 6; Invitrogen), anti-complex IV (cytochrome c oxidase IV; Invitrogen), anti-complex II (succinate dehydrogenase subunit B; Invitrogen), anti-PARP (BD), anti-cleaved PARP (Cell Signaling Technology), anti-Smac/Diablo (BD), and anti-tafazzin (Abcam).

Cell fractionation

HeLa cells were harvested and washed twice in cold PBS. Cells were then washed once in cold mitochondria isolation buffer (MIB; 200 mM mannitol, 70 mM sucrose, 1 mM EGTA, 10 mM Hepes, and 0.05% BSA, pH 7.4). Pellets were then resuspended in 1 ml of MIB and incubated at 4°C for 5 min. The cells were homogenized in Dounce homogenizer. The nuclei were separated and discarded by centrifugation at 750 g for 5 min, and the mitochondria and cytosolic fractions were finally separated by centrifugation at 10,000 g. The mitochondria-enriched fractions were resuspended in a minimal volume of MIB, and the mitochondrial and cytosolic protein concentrations were assessed using the BCA Protein Assay kit (Thermo Fisher Scientific).

In vitro cytochrome c and Smac/Diablo release

Mitochondria were isolated from HeLa or lymphoblastoid cells, as described in "Cell fractionation." Isolated mitochondria were resuspended at 0.5 mg/ml in a reaction buffer (125 mM KCl, 1 mM KH_2PO_4 , 2.5 mM MgCl_2 , 0.2 mM EGTA, 5 mM Hepes, and 0.1% BSA, pH 7.4) in the presence of 10 mM succinate and 1 μ M rotenone. After 5 min incubation at RT, the recombinant tBid protein (a gift from L. Scorrano, University of Padua, Padua, Italy) was added at the indicated concentrations and mitochondria were incubated for 15 min at 37°C. Mitochondria were then collected by centrifugation at 10,000 g for 5 min. Supernatants and pellets were analyzed by immunoblotting.

Protein oligomerization analyses

For the analysis of oligomerization of Bak and/or caspase-8, mitochondria were incubated for 30 min at room temperature in the presence of DMSO (control) or 10 mM BMH (Thermo Fisher Scientific). Mitochondria were then pelleted, and the cross-linking reaction was quenched by addition of NuPAGE sample buffer containing DTT. Pellets were then analyzed by SDS-PAGE in a 4–12% acrylamide gradient gel (NuPAGE; Invitrogen), followed by immunoblotting.

For the analysis of endogenous caspase-8 oligomerization on the mitochondria, cells were trypsinized, washed in PBS, resuspended in cross-linking buffer (210 mM mannitol, 70 mM sucrose, 1 mM EGTA, and 5 mM Hepes, pH 7.4), and permeabilized using 0.05% digitonin (EMD). 10 mM BMH (or DMSO for control) was added, and the permeabilized cells were incubated for 30 min at RT. The cells were then homogenized with a Dounce homogenizer, and mitochondrial fractions were prepared as described in "Cell fractionation." Mitochondrial pellets were resuspended in protein sample buffer containing DTT and analyzed by 4–12% gradient SDS-PAGE (NuPAGE).

Alkaline wash and trypsinization of mitochondrial proteins

Isolated mitochondria were incubated for 30 min at 4°C in MIB buffer containing 0.1 M Na_2CO_3 (pH 11.5). The mitochondrial membranes, containing the integrated proteins, were pelleted by ultracentrifugation at 100,000 g for 30 min at 4°C. The supernatants were also collected. Both fractions were then analyzed by Western blotting. The efficiency of the alkaline extraction was controlled using two mitochondrial proteins, NADH-dehydrogenase subunit 6 (an integral membrane protein) and succinate dehydrogenase subunit B (loosely associated to the matrix side of the mitochondrial inner membrane).

The susceptibility of mitochondria-associated caspase-8 to trypsin digestion was checked by isolating mitochondria from HeLa cells transiently expressing caspase-8-C360S-GFP in the presence of zVAD-fmk (EMD). Isolated mitochondria were resuspended in trypsin digestion buffer and incubated with various concentrations of trypsin (Sigma-Aldrich) for 20 min on ice. The proteolysis was stopped by the addition of a 10-fold excess of soybean trypsin inhibitor (Sigma Aldrich). Mitochondria were pelleted at 100,000 g for 30 min at 4°C and analyzed by immunoblotting.

Liposome preparation and analysis

The lipid composition of liposomes was based on the composition of mitochondrial contact sites as described previously (Lutter et al., 2000). Liposomes containing CL consisted of 41 mol% (molar percentage) PC,

22 mol% PE, 8 mol% PI, 9 mol% cholesterol, and 20 mol% CL. In the liposomes lacking CL, we increased both the PC and PE content to compensate for the lack of CL. Bovine liver PC, PE, and PI were obtained from Avanti Polar Lipids, Inc., and bovine heart CL (~98% pure, >80% polyunsaturated fatty acids, primarily linoleic acid) and cholesterol were obtained from Sigma-Aldrich. For the preparation of the liposomes, lipids were dissolved in chloroform, dried under nitrogen, and resuspended in binding buffer containing 100 mM NaCl, 2 mM MgCl₂, and 10 mM Tris, pH 7.1. The lipid mixture was passed 11 times through a 400-nm polycarbonate membrane of a Mini-Extruder (Avanti Polar Lipids, Inc.) to form large unilamellar vesicles. After precipitation and wash of liposomes at 100,000 g for 15 min at 4°C, the presence or absence of CL was confirmed by mass spectrometry analysis. The indicated proteins were incubated with the liposomes in binding buffer at 37°C for 30 min, and liposomes were then centrifuged, washed in binding buffer, 0.1 M Na₂CO₃, pH 11.5, or 1 M NaCl, and lysed for protein analysis by immunoblotting.

Online supplemental material

Fig. S1 shows the Fas expression for all lymphoblastoid cell lines. Fig. S2 shows the effect of siBid or Bcl-X_L on anti-Fas stimulated cell death in HeLa cells. Fig. S3 shows the mRNA expression levels of tafazzin in the tafazzin knockdown HeLa cells compared with controls. Fig. S4 shows the lipid content of shCont1, shCont2, shTaz1, and shTaz2. Fig. S5 shows the expression of and localization of tafazzin-GFP and that transient knockdown of tafazzin did not alter CL levels or prevent cell death induced by anti-Fas antibody. Online supplemental material is available at <http://www.jcb.org/cgi/content/full/jcb.200803129/DC1>.

We thank Wouter Visser for excellent technical assistance with liposomes preparation, and Ayala King for excellent editorial work.

This work was supported by Cancer Research UK. F.M. Vaz was supported by Prinses Beatrix Fonds (grant No. WAR05-0126) and by the Barth Syndrome Foundation. P.X. Petit was supported by the Association Française contre les Myopathies (grant No. 11557). The generation of Barth syndrome lymphoblastoid cells was supported by National Institute of Child Health and Human Development Mental Retardation Research Center grant No. HD-2406.

Submitted: 25 March 2008

Accepted: 22 October 2008

References

Ardail, D., J.P. Privat, M. Egret-Charlier, C. Levrat, F. Lerme, and P. Louisot. 1990. Mitochondrial contact sites. Lipid composition and dynamics. *J. Biol. Chem.* 265:18797–18802.

Barth, P.G., H.R. Scholte, J.A. Berden, J.M. Van der Klei-Van Moorsel, I.E. Luyt-Houwen, E.T. Van 't Veer-Korthof, J.J. Van der Harten, and M.A. Sobotka-Pløjhar. 1983. An X-linked mitochondrial disease affecting cardiac muscle, skeletal muscle and neutrophil leucocytes. *J. Neurol. Sci.* 62:327–355.

Bione, S., P. D'Adamo, E. Maestrini, A.K. Gedeon, P.A. Bolhuis, and D. Toniolo. 1996. A novel X-linked gene, G4.5, is responsible for Barth syndrome. *Nat. Genet.* 12:385–389.

Bleyle, S.B., B.R. Mumford, V. Thompson, J.C. Carey, T.J. Pysher, T.K. Chin, and K. Ward. 1997. Neonatal, lethal noncompaction of the left ventricular myocardium is allelic with Barth syndrome. *Am. J. Hum. Genet.* 61:868–872.

Chandra, D., G. Choy, X. Deng, B. Bhatia, P. Daniel, and D.G. Tang. 2004. Association of active caspase 8 with the mitochondrial membrane during apoptosis: potential roles in cleaving BAP31 and caspase 3 and mediating mitochondrion-endoplasmic reticulum cross talk in etoposide-induced cell death. *Mol. Cell. Biol.* 24:6592–6607.

Chang, D.W., Z. Xing, V.L. Capacio, M.E. Peter, and X. Yang. 2003. Inter-dimer processing mechanism of procaspase-8 activation. *EMBO J.* 22:4132–4142.

Chen, M., A. Orozco, D.M. Spencer, and J. Wang. 2002. Activation of initiator caspases through a stable dimeric intermediate. *J. Biol. Chem.* 277:50761–50767.

Choi, S.Y., F. Gonzalez, G.M. Jenkins, C. Slomianny, D. Chretien, D. Arnoult, P.X. Petit, and M.A. Frohman. 2007. Cardiolipin deficiency releases cytochrome c from the inner mitochondrial membrane and accelerates stimuli-elicited apoptosis. *Cell Death Differ.* 14:597–606.

Donepudi, M., A. Mac Sweeney, C. Briand, and M.G. Grutter. 2003. Insights into the regulatory mechanism for caspase-8 activation. *Mol. Cell.* 11:543–549.

Esposti, M.D., I.M. Cristea, S.J. Gaskell, Y. Nakao, and C. Dive. 2003. Proapoptotic Bid binds to monolysocardiolipin, a new molecular connection between mitochondrial membranes and cell death. *Cell Death Differ.* 10:1300–1309.

Gonzalvez, F., and E. Gottlieb. 2007. Cardiolipin: Setting the beat of apoptosis. *Apoptosis.* 12:877–885.

Gonzalvez, F., J.J. Bessoule, F. Rocchiccioli, S. Manon, and P.X. Petit. 2005a. Role of cardiolipin on tBid and tBid/Bax synergistic effects on yeast mitochondria. *Cell Death Differ.* 12:659–667.

Gonzalvez, F., F. Pariselli, P. Dupaigne, I. Budihardjo, M. Lutter, B. Antonsson, P. Dirolez, S. Manon, J.C. Martinou, M. Goubern, et al. 2005b. tBid interaction with cardiolipin primarily orchestrates mitochondrial dysfunctions and subsequently activates Bax and Bak. *Cell Death Differ.* 12:614–626.

Hauff, K.D., and G.M. Hatch. 2006. Cardiolipin metabolism and Barth syndrome. *Prog. Lipid Res.* 45:91–101.

Hovius, R., H. Lambrechts, K. Nicolay, and B. de Kruijff. 1990. Improved methods to isolate and subfractionate rat liver mitochondria. Lipid composition of the inner and outer membrane. *Biochim. Biophys. Acta.* 1021:217–226.

Kagan, V.E., V.A. Tyurin, J. Jiang, Y.Y. Tyurina, V.B. Ritov, A.A. Amoscato, A.N. Osipov, N.A. Belikova, A.A. Kapralov, V. Kini, et al. 2005. Cytochrome c acts as a cardiolipin oxygenase required for release of proapoptotic factors. *Nat. Chem. Biol.* 1:223–232.

Kelley, R.I., J.P. Cheatham, B.J. Clark, M.A. Nigro, B.R. Powell, G.W. Sherwood, J.T. Sladky, and W.P. Swisher. 1991. X-linked dilated cardiomyopathy with neutropenia, growth retardation, and 3-methylglutaconic aciduria. *J. Pediatr.* 119:738–747.

Kim, T.H., Y. Zhao, W.X. Ding, J.N. Shin, X. He, Y.W. Seo, J. Chen, H. Rabinovich, A.A. Amoscato, and X.M. Yin. 2004. Bid-cardiolipin interaction at mitochondrial contact site contributes to mitochondrial cristae reorganization and cytochrome C release. *Mol. Biol. Cell.* 15:3061–3072.

Kischkel, F.C., S. Hellbardt, I. Behrmann, M. Germer, M. Pawlita, P.H. Kramer, and M.E. Peter. 1995. Cytotoxicity-dependent APO-1 (Fas/CD95)-associated proteins form a death-inducing signaling complex (DISC) with the receptor. *EMBO J.* 14:5579–5588.

Kobayashi, T., M. Yamaguchi, S. Kim, J. Morikawa, S. Ogawa, S. Ueno, E. Suh, E. Dougherty, I. Shmulevich, H. Shiku, and W. Zhang. 2003. Microarray reveals differences in both tumors and vascular specific gene expression in de novo CD5+ and CD5- diffuse large B-cell lymphomas. *Cancer Res.* 63:60–66.

Kuwana, T., M.R. Mackey, G. Perkins, M.H. Ellisman, M. Latterich, R. Schneider, D.R. Green, and D.D. Newmeyer. 2002. Bid, bax, and lipids cooperate to form supramolecular openings in the outer mitochondrial membrane. *Cell.* 111:331–342.

Landriscina, C., F.M. Megli, and E. Quagliariello. 1976. Turnover of fatty acids in rat liver cardiolipin: comparison with other mitochondrial phospholipids. *Lipids.* 11:61–66.

Li, H., H. Zhu, C.J. Xu, and J. Yuan. 1998. Cleavage of BID by caspase 8 mediates the mitochondrial damage in the Fas pathway of apoptosis. *Cell.* 94:491–501.

Liu, J., A. Weiss, D. Durrant, N.W. Chi, and R.M. Lee. 2004. The cardiolipin-binding domain of Bid affects mitochondrial respiration and enhances cytochrome c release. *Apoptosis.* 9:533–541.

Liu, J., D. Durrant, H.S. Yang, Y. He, F.G. Whitty, D.G. Myszka, and R.M. Lee. 2005. The interaction between tBid and cardiolipin or monolysocardiolipin. *Biochem. Biophys. Res. Commun.* 330:865–870.

Luo, X., I. Budihardjo, H. Zou, C. Slaughter, and X. Wang. 1998. Bid, a Bcl2 interacting protein, mediates cytochrome c release from mitochondria in response to activation of cell surface death receptors. *Cell.* 94:481–490.

Lutter, M., M. Fang, X. Luo, M. Nishijima, X. Xie, and X. Wang. 2000. Cardiolipin provides specificity for targeting of tBid to mitochondria. *Nat. Cell Biol.* 2:754–761.

Lutter, M., G.A. Perkins, and X. Wang. 2001. The pro-apoptotic Bcl-2 family member tBid localizes to mitochondrial contact sites. *BMC Cell Biol.* 2:22.

Martinou, F., K. Burns, and J. Tschoopp. 2002. The inflammasome: a molecular platform triggering activation of inflammatory caspases and processing of proIL-beta. *Mol. Cell.* 10:417–426.

Milovic-Holm, K., E. Kriehoff, K. Jensen, H. Will, and T.G. Hofmann. 2007. FLASH links the CD95 signaling pathway to the cell nucleus and nuclear bodies. *EMBO J.* 26:391–401.

Ott, M., J.D. Robertson, V. Gogvadze, B. Zhivotovsky, and S. Orrenius. 2002. Cytochrome c release from mitochondria proceeds by a two-step process. *Proc. Natl. Acad. Sci. USA.* 99:1259–1263.

Scaffidi, C., S. Fulda, A. Srinivasan, C. Friesen, F. Li, K.J. Tomaselli, K.M. Debatin, P.H. Kramer, and M.E. Peter. 1998. Two CD95 (APO-1/Fas) signaling pathways. *EMBO J.* 17:1675–1687.

- Shell, S., S.M. Park, A.R. Radjabi, R. Schickel, E.O. Kistner, D.A. Jewell, C. Feig, E. Lengyel, and M.E. Peter. 2007. Let-7 expression defines two differentiation stages of cancer. *Proc. Natl. Acad. Sci. USA*. 104:11400–11405.
- Shidoji, Y., K. Hayashi, S. Komura, N. Ohishi, and K. Yagi. 1999. Loss of molecular interaction between cytochrome c and cardiolipin due to lipid peroxidation. *Biochem. Biophys. Res. Commun.* 264:343–347.
- Simbeni, R., L. Pon, E. Zinser, F. Paltauf, and G. Daum. 1991. Mitochondrial membrane contact sites of yeast. Characterization of lipid components and possible involvement in intramitochondrial translocation of phospholipids. *J. Biol. Chem.* 266:10047–10049.
- Slee, E.A., M.T. Harte, R.M. Kluck, B.B. Wolf, C.A. Casiano, D.D. Newmeyer, H.G. Wang, J.C. Reed, D.W. Nicholson, E.S. Alnemri, et al. 1999. Ordering the cytochrome c-initiated caspase cascade: hierarchical activation of caspases-2, -3, -6, -7, -8, and -10 in a caspase-9-dependent manner. *J. Cell Biol.* 144:281–292.
- Stegh, A.H., H. Herrmann, S. Lampel, D. Weisenberger, K. Andra, M. Seper, G. Wiche, P.H. Kramer, and M.E. Peter. 2000. Identification of the cytolinker plectin as a major early in vivo substrate for caspase 8 during CD95- and tumor necrosis factor receptor-mediated apoptosis. *Mol. Cell. Biol.* 20:5665–5679.
- Stegh, A.H., B.C. Barnhart, J. Volkland, A. Algeciras-Schimmich, N. Ke, J.C. Reed, and M.E. Peter. 2002. Inactivation of caspase-8 on mitochondria of Bcl-xL-expressing MCF7-Fas cells: role for the bifunctional apoptosis regulator protein. *J. Biol. Chem.* 277:4351–4360.
- Stupack, D.G., T. Teitz, M.D. Potter, D. Mikolon, P.J. Houghton, V.J. Kidd, J.M. Lahti, and D.A. Cheresch. 2006. Potentiation of neuroblastoma metastasis by loss of caspase-8. *Nature*. 439:95–99.
- Tinel, A., and J. Tschopp. 2004. The PIDosome, a protein complex implicated in activation of caspase-2 in response to genotoxic stress. *Science*. 304:843–846.
- Tu, S., G.P. McStay, L.M. Boucher, T. Mak, H.M. Beere, and D.R. Green. 2006. In situ trapping of activated initiator caspases reveals a role for caspase-2 in heat shock-induced apoptosis. *Nat. Cell Biol.* 8:72–77.
- Valianpour, F., R.J. Wanders, H. Overmars, P. Vreken, A.H. Van Gennip, F. Baas, B. Plecko, R. Santer, K. Becker, and P.G. Barth. 2002. Cardiolipin deficiency in X-linked cardioskeletal myopathy and neutropenia (Barth syndrome, MIM 302060): a study in cultured skin fibroblasts. *J. Pediatr.* 141:729–733.
- Valianpour, F., V. Mitsakos, D. Schlemmer, J.A. Towbin, J.M. Taylor, P.G. Ekert, D.R. Thorburn, A. Munnich, R.J. Wanders, P.G. Barth, and F.M. Vaz. 2005. Monolysocardiolipins accumulate in Barth syndrome but do not lead to enhanced apoptosis. *J. Lipid Res.* 46:1182–1195.
- van Loo, G., X. Saelens, M. van Gurp, M. MacFarlane, S.J. Martin, and P. Vandenabeele. 2002. The role of mitochondrial factors in apoptosis: a Russian roulette with more than one bullet. *Cell Death Differ.* 9:1031–1042.
- Varfolomeev, E.E., M. Schuchmann, V. Luria, N. Chiannikulchai, J.S. Beckmann, I.L. Mett, D. Rebrikov, V.M. Brodianski, O.C. Kemper, O. Kollet, et al. 1998. Targeted disruption of the mouse caspase 8 gene ablates cell death induction by the TNF receptors, Fas/Apo1, and DR3 and is lethal prenatally. *Immunity*. 9:267–276.
- Vreken, P., F. Valianpour, L.G. Nijtmans, L.A. Grivell, B. Plecko, R.J. Wanders, and P.G. Barth. 2000. Defective remodeling of cardiolipin and phosphatidylglycerol in Barth syndrome. *Biochem. Biophys. Res. Commun.* 279:378–382.
- Wang, X. 2001. The expanding role of mitochondria in apoptosis. *Genes Dev.* 15:2922–2933.
- Wilson, K.S., H. Roberts, R. Leek, A.L. Harris, and J. Geradts. 2002. Differential gene expression patterns in HER2/neu-positive and -negative breast cancer cell lines and tissues. *Am. J. Pathol.* 161:1171–1185.
- Xu, Y., A. Malhotra, M. Ren, and M. Schlame. 2006. The enzymatic function of tafazzin. *J. Biol. Chem.* 281:39217–39224.
- Zhang, X., L. Li, J. Choe, S. Krajewski, J.C. Reed, C. Thompson, and Y.S. Choi. 1996. Up-regulation of Bcl-xL expression protects CD40-activated human B cells from Fas-mediated apoptosis. *Cell. Immunol.* 173:149–154.
- Zhang, H., Q. Xu, S. Krajewski, M. Krajewska, Z. Xie, S. Fuess, S. Kitada, K. Pawlowski, A. Godzik, and J.C. Reed. 2000. BAR: An apoptosis regulator at the intersection of caspases and Bcl-2 family proteins. *Proc. Natl. Acad. Sci. USA*. 97:2597–2602.
- Zou, H., Y. Li, X. Liu, and X. Wang. 1999. An APAF-1-cytochrome c multimeric complex is a functional apoptosome that activates procaspase-9. *J. Biol. Chem.* 274:11549–11556.